AN ABSTRACT OF THE THESIS OF

Dongtai Liu for the degree of Doctor of Philosophy in Electrical and Computer Engineering presented on December 5, 1990 .

Title: OptoNet - A Non-directional Infrared Communication Link for Local Area Networks

Abstract approved: Redacted for privacy

James H. Herzog

This thesis work researches the theory and application of systems performing omnidirectional, non-direct path optical data communication (ONP systems). Such systems are characterized by 1) the communication involves a local, usually circular area; 2) Obstacles are allowed between a transmitter and the receivers. This is in contrast to the point-to-point and line-of-sight communications performed by almost all existing infrared data communication or transmission systems. The elimination of the point-to-point limitation makes ONP systems suitable for optical local area networking.

The feasibility of ONP systems employing infrared LEDs and silicon photo detectors has been analyzed and the performance of such systems predicted. The analysis shows that indoor ONP systems are both feasible and practical. Only a few LEDs are required to cover the entire area of a large room.

Efforts have been made in finding rules for optimal design of the ONP systems. A set of design criteria and

curves have been established.

The theoretical analysis has been verified in a successful experiment done with OptoNet, an ONP infrared datalink for local area networks. This experimental system consists of two identical communication units employing FSK modulation and microprocessor controllers. The experiment has demonstrated that the ONP optical data communications can be realized by relatively simple electronic hardware.

OptoNet -
A Non-directional Infrared Communication Link For Local Area Networks

by

Dongtai Liu

A THESIS
submitted to
Oregon State University

in partial fulfillment of
the requirements for the
degree of

Doctor of Philosophy

Completed December 5th, 1990
Commencement June, 1991

APPROVED:

Redacted for privacy

Associate professor in charge of major

Redacted for privacy

Head of department of Electrical & Computer Engineering

Redacted for privacy

Dean of Graduate School

Date thesis is presented: December 5, 1990

Name of Student: Dongtai Liu

ACKNOWLEDGEMENTS

I would like to extend my sincere thanks to Dr. James H. Herzog, my major professor, for his encouragement and guidance throughout this study.

I would like thank Mr. Paul Davis, the president of Videx, Inc., for his generous support in providing test facillities for my experiments.

I warmly thank all of my friends and colleagues whose assistance and encouragement has been invaluable.

TABLE OF CONTENTS

LIST OF FIGURES

OptoNet -
A Non-directional Infrared Communication Link
For Local Area Networks

CHAPTER ONE

INTRODUCTION TO OMNIDIRECTIONAL AND NON-DIRECT PATH INFRARED OPTICAL DATA COMMUNICATION

The use of infrared (IR) light as a free space data communication carrier has gained considerable interest in recent years. Infrared data communications are characterized by safety, wirelessness, signal locality, and invisibility. Another advantage is that in most countries infrared communication is not regulated by the government; hence they are suitable for a wide variety of applications.

Free space optical data communication systems can be characterized by different forms of optical paths and radiation patterns. The optical path can be direct (line-of-light) or non-direct (by reflection). The radiation pattern can be a focused beam or cone, or it can be omnidirectional. Therefore there are four possible combinations. The focused and direct path system (or abbreviated as the FDP system) is the prevailing type in most application. The other potentially useful type is the omni-directional and non-direct path system, abbreviated as the ONP system. In an ONP system, light energy is radiated from the transmitter omnidirectionally and reaches the receiver from all directions via direct paths or by reflection off the ceiling and walls.

Two types of semiconductor devices are suitable for

use as infrared light sources, infrared light emitting diodes (infrared LED) and infrared laser diodes. Laser diodes have very fast response time (nanoseconds), small output power and low efficiency. Infrared LED's have relatively slow response (microseconds), large output power and high efficiency. Different radiating cone angles are available for the LEDs. Other infrared light sources, such as the gas lasers, are not suitable because their intensity cannot be controlled effectively for modulation, or their efficiency are two low.

According to the author's knowledge, almost all free space optical data communication systems now in use belong to the FDP system class. They range from TV remote controls, where loose focus is used, to the laser code reader, where sharp focus is used. FDP type optical computer data link products have also emerged recently. FDP systems prevail because their signal level is relatively high due to the direct line of sight and focusing. Therefore, relatively simple, low cost techniques can be used to achieve the required range and data security. Due to the focusing and line-of-sight requirement, FDP systems require physical alignment of the transmitter and the receiver.

An example of FDP computer data link system is the Photo Link Cabling System developed by Photonics in 1989 [1]. It is designed for open office environments. It consists of a "Photolink" which connects to up to 4 personal computers. The Photolink is mounted in a high location and transmits and receives focused infrared beams. It is designed as a point to point cable replacement and cannot be used as a LAN. Another example is an optical keyboard designed by Three-Five System Inc. It is a semi-focused optical data communication system

with a narrow infrared beam cone angle of 16 degrees [2].

On the other hand, there has been little study on ONP systems. The author has done a computer aided library search and found no publications on similar topic. ONP systems offer some significant advantages over FDP systems. Since both the light emission and reception are omnidirectional and the ceiling and walls are used as reflectors, there are no problems related to physical alignment and placement. The large coverage of the communication area also makes multidrop optical communication networks possible.

The difficulty in realizing a ONP system lies in the low signal level which results in a poor signal-to-noise ratio. The light beams are diffused after reflection and fill the entire room. The light flux density at any point in the area is very low. Only a tiny fraction of the total emitted power can be collected by the photo detector which usually has an effective detecting area of only a few square millimeters. The poor reflectance ratio of most building materials makes the situation even worse. Therefore, the key point of a realization involving ONP is to achieve the highest possible system efficiency. In multidrop networking situations the collision problem caused by the simultaneous transmission of multiple network nodes will also have to be solved.

The scope of this thesis work is to research the theory and practice of ONP free space indoor optical data communication. The limits of such systems are to be determined analytically and verified experimentally. Specifically, the following aspects will be addressed in Chapter Two through Chapter Five:

- Illumination functions for FDP and ONP systems
- ONP feasibility study
- Analysis of optimal LED driving methods
- System level design considerations
- Experiment and verification of ONP optical communication

In Chapter Two the illumination functions for the FDP and ONP systems are derived. The two classes of systems are compared analytically with respect to their relative signal level using the illumination functions. The extremely weak signal level of the ONP system raises the question of its feasibility. Much more emitted power from the ONP transmitter (meaning increased cost and power) seems to be required for a ONP receiver to obtain a similar signal level to that obtained in a FDP system.

Chapter Three addresses the feasibility question by calculating the ONP communication range as a function of the total emitted light power. The calculation shows that in an ideal system only a few infrared LED's are needed to cover a large room for ONP communication. ONP would be feasible if a properly designed system with high efficiency were available.

Chapter Four investigates on the LED driver stage which has a great effect on the transmitter's power efficiency. A thorough analysis of the power efficiency was performed. This produced a set of curves showing the

relationship between data rate, communication range and emitted light power. Given predefined requirements, the curves help to find optimal system parameters in the sense of energy conversion efficiency.

Chapter Five includes an example of the design and implementation of an ONP free space indoor optical data communication system. The methodology developed in Chapter Four and some radio frequency principles are used in the design.

CHAPTER TWO
THE ANALYSIS OF ILLUMINATION FUNCTIONS

In a free space optical data communication system, light energy is used as the data carrier. Normally the light source is modulated in intensity to encode the information to be transmitted. This variation of intensity is detected by the receiver and is converted back to electrical signals.

In an unfocused or semifocused free space optical communication system, the optical signal level attenuates rapidly with distance. The strength of the optical signal is measured by its flux (optical power) density on a surface in the units of watt/m^2. The flux density of a point on a surface exposed to incident light is called *Radiant Incidance,* or *Illumination.* The function that describes the change of illumination on a surface is called the *Illumination Function.* The illumination function is very important in the analysis of a free space optical communication system. For an ONP system, we are particularly interested in the *Floor Illumination Function*, which can be used to calculate the optical power received by a photo detector placed on the "floor", an imaginary plane facing the ceiling.

In the following sections the illumination functions for the FDP and ONP systems will be derived. Although the primary interest is in finding the floor illumination function for the ONP system, the illumination function for the FDP system will be derived as well in order to be

able to compare the two systems quantitatively. The terms and units that will be used are those recommended by the Optical Society of America [3]. Table I summarizes these quantities that will appear subsequently.

TABLE 2.1 RADIOMETRIC SYMBOLS, NAMES AND UNITS

Symbol and Equation	Name	Description	Unit
U	Radiant energy		joule
$\Phi=dU/dt$	Radiant power (flux)	Rate of transfer of radiant energy	watt
$W=d\Phi/ds$	Radiant flux density	Radiant power incident on or leaving a surface, divided by the area of that surface	watt/cm^2
$E=d\Phi/ds$	Radiant incidance	Radiant flux density incident upon a surface	watt/cm^2
$M=d\Phi/ds$	Radiant exitance	Radiant flux density leaving a surface	watt/cm^2
$I=d\Phi/d\Omega$	Radiant intensity	Radiant power leaving a point source per unit solid angle	watt/sr
μ	Radiant reflectance	Ratio of absorbed radiant power to incidant radiant power	

2.1 The Illumination Function for FDP Systems

The typical radiant pattern of a FDP free-space optical data communication system is illustrated by Figure 2.1. The transmission efficiency EFF_t is defined as the ratio of the power received by the photo detector to the power emitted by the LED. To evaluate the transmission efficiency of the FDP system it is convenient to use the concept of solid angle.

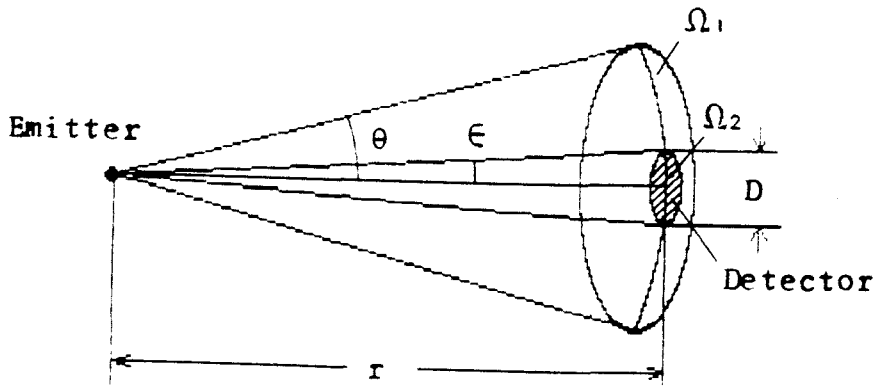

Figure 2.1 A FDP system

For simplicity the radiant intensity of the LED is assumed to be uniform over the entire solid angle Ω_1 having a half cone angle of θ. (Appendix B illustrates the radiant intensity patterns of an actual LED). Since the radiant intensity is the same everywhere within θ, the transmission efficiency is then the ratio of Ω_1 to Ω_2, where Ω_2 is the solid angle of the cone formed by the

effective detecting surface and the vertex with half cone angle of ϵ.

$$\Omega_1 = 2\pi(1-\cos\theta)$$
$$= 4\pi\sin^2(\theta/2)$$

$$\Omega_2 = 2\pi(1-\cos\epsilon)$$
$$= 4\pi\sin^2(\epsilon/2)$$

since ϵ is very small, $\sin(\epsilon/2)$ can be approximated by $\frac{1}{4}(D/r)$ where r is the distance between the LED and the photo detector, and D is the diameter of the effective detecting area of the photo detector. Therefore,

$$\Omega_2 = \tfrac{1}{4}\pi(D/r)^2$$

the transmission efficiency is then

$$EFF_t = \frac{\Omega_2}{\Omega_1}$$

$$= \frac{\frac{1}{4}\pi(D/r)^2}{4\pi\sin^2(\theta/2)}$$

Example 2.1

In FDP systems, narrow beam LEDs are usually used. As an example, let $\theta=10^\circ$, r=10m and D=2.5mm.

$$EFF_t = \frac{\frac{1}{4}\pi(0.0025/10)^2}{4\pi\sin^2(10^\circ/2)} \qquad (2\text{-}1)$$

$$= 0.51\text{x}10^{-6}$$

In this case, approximately half a millionth of the total emitted power is received by the detector at a distance of 10 meters.

Example 2.2

Assume that a focused laser diode is used with $\theta=1^\circ$, r=10m and D=2.5mm.

$$EFF_t = \frac{\frac{1}{4}\pi(0.0025/10)^2}{4\pi\sin^2(1^\circ/2)}$$

$$= 0.515\text{x}10^{-4}$$

An improvement in coupling efficiency by a factor of 100 is gained by narrowing the light beam by a factor of 10. In general, if θ is 10° or less the coupling efficiency is approximately inversely proportional to the square of θ.

2.2. The Floor Illumination Function for ONP Systems

In a ONP system, line-of-sight does not exist between the light emitter and the photodetector. The transmission of light mainly depends on the ceiling which acts as a

diffuse reflector. Every area on the ceiling contributes to the illumination of the receiver. Therefore the illumination level of the receiver is an integration of such contributions over the entire ceiling.

In determining the illumination of a point at a random location on the floor, the following assumptions are made:

1. Both the emitter and detector are placed on the floor plane. The emitter radiates omni-directioanlly in the upper hemisphere. The detector also receives omnidirectioanlly in the upper hemisphere.

2. The ceiling is a diffuse reflector having a reflectance ratio μ;

3. The floor is a non-reflectant plane parallel to the ceiling;

4. Both the ceiling and floor planes are infinite and the reflection off the walls are neglected;

5. There is a small opaque object blocking the line-of-sight between the emitter and detector. The effect of the its shadow on the ceiling illumination is negligible.

Assumption (4) merits some discussion. For a large room where the width and depth of the room is much greater than the height of the ceiling, only a very small portion of the reflected power is received from the walls and the assumption is a good approximation. For a small room, the walls would strengthen the signal level. Therefore (4)

represents a worst case condition.

First, $M(\Phi,h,r,\mu)$, the *radiant exitance* of any point on the ceiling as a function of the total emitted optical power, the height of the ceiling, the distance from the emitter to the receiver and the ceiling's reflectant ratio will be found . Then, $E_f(\Phi,h,r,\mu)$, the floor illumination function, the equation that can be used to calculate the *radiant incidance* at any point on the floor will be derived. Knowing the radiant incidance at any point on the floor, the amount of optical power that a photo detector receives can then be quantitatively determined.

2.2.1 Ceiling Radiant Exitance Function

A typical ONP system is illustrated by Figure 2.2. The figure is drawn in two dimensions since everything is symmetrical about the vertical axis passing through the emitter.

The incident radiant flux density (illumination) on the ceiling E_c, and the radiant exitance function (flux

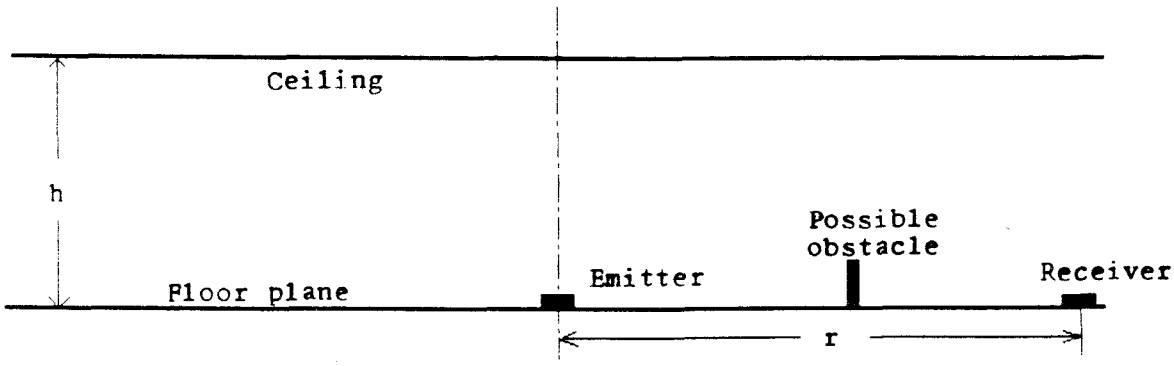

Figure 2.2
An ONP system

reflected off the ceiling per unit area) are denoted by E_c and M_c, respectively, and $M_c=\mu E_c$.

E_c is a function of the total emitted power Φ, the height of the ceiling h and the horizontal distance r and satisfies the following relation:

$$E_c(\Phi,r,h) = \frac{h/2\pi}{(h^2+r^2)^{3/2}}\cdot\Phi \qquad \text{watt/m}^2 \qquad (2\text{-}2)$$

Proof 1

Since the omnidirectional emitter can be considered a point source, $E'_c(\Phi,r,h)$, the illumination of a small surface on the ceiling perpendicular to the incident light (Figure 2.3), is inversely proportional to the square of the distance:

$$E'_c(\Phi,r,h) = \frac{A(\Phi)}{h^2+r^2} \qquad \text{watt/m}^2$$

where $A(\Phi)$ is some linear function of the total emitted power Φ.

A small surface on the ceiling has a downward vertical normal which makes an angle α with the incident light. Therefore the illumination of point a is the scalar product of $E'_c(\Phi,r,h)$ and the normal of ceiling:

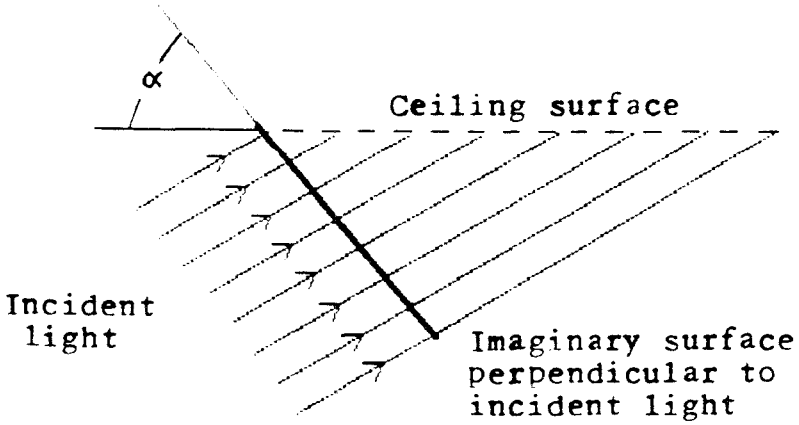

Figure 2.3

Perpendicular Incident Flux Density

$$E_c(\Phi,r,h) = \frac{A(\Phi)}{h^2+r^2}\cdot\cos(\alpha)$$

$$= \frac{A(\Phi)}{h^2+r^2}\cdot\frac{h}{\sqrt{h^2+r^2}}$$

$$= \frac{A(\Phi)\cdot h}{(h^2+r^2)^{3/2}} \qquad (\text{watt}/\text{m}^2) \qquad (2\text{-}3)$$

To find $A(\Phi)$ we just need to equate the total emitted power Φ and the total flux passing an infinitely large ceiling. The latter is the integral of the flux density over the entire ceiling:

$$\Phi = \int_{s->\infty} E_c(\Phi, r, h)\, ds$$

$$= \int_{s->\infty} \frac{A(\Phi)\ h}{(h^2 + r^2)^{3/2}}\, ds$$

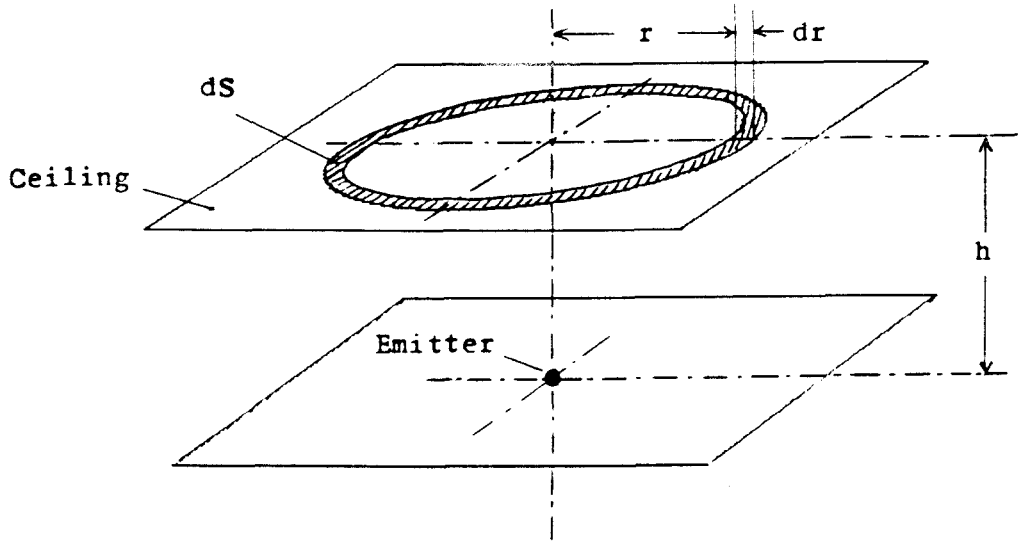

Figure 2.4
the differential of area S

using the polar form of ds as shown by Figure 2.4, the integral can be written as

$$\Phi = \int_{r=0}^{\infty} \frac{2\pi \cdot A(\Phi) \cdot h}{(h^2+r^2)^{3/2}} \, rdr$$

$$= \pi h A(\Phi) \int_{r=0}^{\infty} \frac{1}{(h^2+r^2)^{3/2}} \, d(r^2)$$

$$= \pi h A(\Phi) \int_{r=0}^{\infty} \frac{1}{(h^2+r^2)^{3/2}} \, d(r^2+h^2)$$

$$= -2\pi h A(\Phi) [1/\sqrt{h^2+r^2}]_{r=0}^{\infty}$$

$$= 2\pi A(\Phi)$$

Therefore,

$$A(\Phi) = \Phi/2\pi$$

Substituting (2-3) for $A(\Phi)$, we obtain the illumination function of the ceiling:

$$Ec(\Phi, r, h) = \frac{h/2\pi}{(h^2+r^2)^{3/2}} \Phi$$

Proof 2

Using the concept of solid angle, the solid angle differential corresponding to ds in Figure 2.3 is

$$d\Omega = \frac{\cos(\alpha)}{r^2+h^2}\, ds$$

$$= \frac{h}{(h^2+r^2)^{3/2}}\, ds$$

since the upper half hemisphere contains a solid angle of 2π, the flux differential contained in $d\Omega$ is

$$d\Phi = \frac{d\Omega}{2\pi}\cdot\Phi$$

$$= \frac{h/2\pi}{(h^2+r^2)^{3/2}}\cdot\Phi\cdot ds$$

therefore,

$$E_c(\Phi,r,h) = \frac{d\Phi}{ds}$$

$$= \frac{h/2\pi}{(h^2+r^2)^{3/2}}\cdot\Phi$$

This quantity is the radiant incidance or the incident light flux density at an arbitrary point on the ceiling. The radiant exitance, or the reflected light flux density $M(\Phi,h,r,\mu)$, is the portion of the incident amount determined by the surface's reflectant ratio μ:

$$M(\Phi,h,r,\mu) = \mu E(\Phi,r,h)$$

$$= \frac{\mu h/2\pi}{(h^2+r^2)^{3/2}} \cdot \Phi \qquad (2\text{-}3)$$

This function is plotted in two ways by Figure 2.5 and Figure 2.6, respectively.

2.2.2 Derivation of the Floor Illumination Function

As the light from the emitter reaches the ceiling, the entire ceiling is illuminated according to the ceiling exitance function $M(\Phi,h,r,\mu)$. Any point on the floor, in

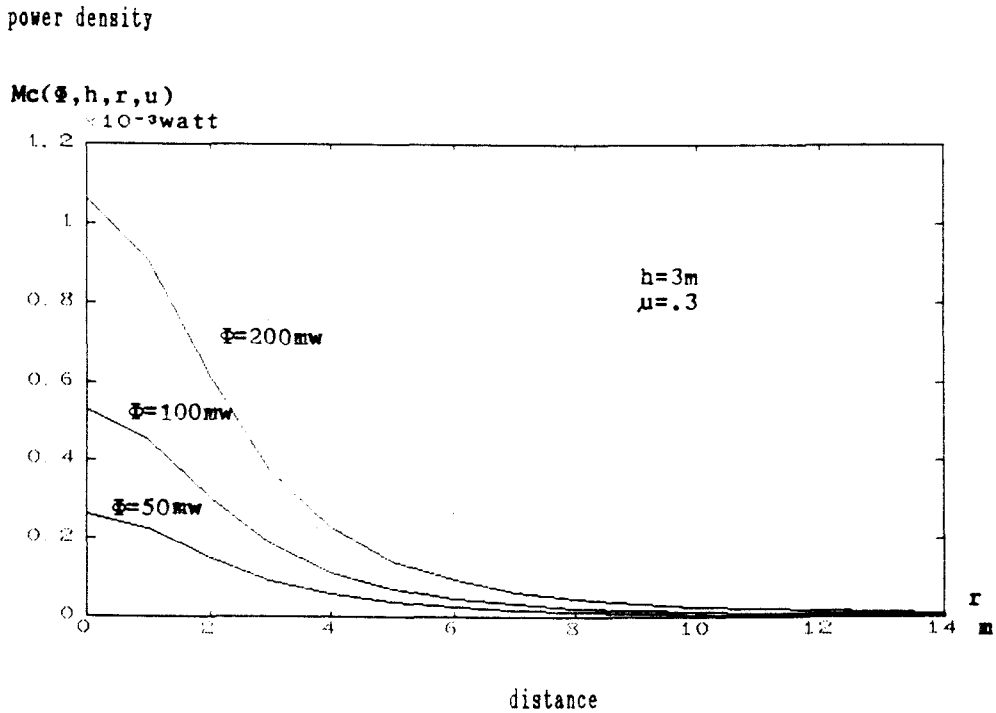

Figure 2.5

Ceiling radiance power density as a function of distance from ceiling center

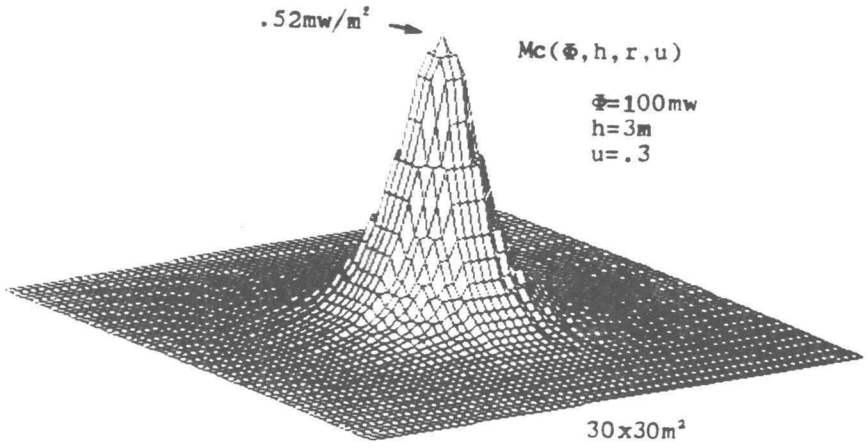

Figure 2.6
Ceiling radiance power density over a 30x30m² ceiling plane

turn, is illuminated by energy originating from every the ceiling surface. The floor illumination function is an integration of the ceiling radiant exitance function $M(\Phi,h,r,\mu)$ over the entire ceiling. We denote the floor illumination function by $E_f(\Phi,h,r,\mu)$. To find E_f we need to find the differential of the radiant incidance for an arbitrary point on the floor plane.

Consider a small ceiling surface element, dS_1, and a small floor surface element, dS_2 (Figure 2.7). The exitant flux differential of dS_1 is denoted by $d\Phi_1$. The incident flux differential of dS_2 is denoted by $d\Phi_2$. The incident

flux density (radiant incidance) differential is denoted by dE_f. Since the distance between the two surfaces is much greater than the diameter of both surfaces, dS_1 can be considered as a point source viewed from dS_2 and the Lambert Cosine Law applies:

$$I(\theta) = I(0)\cdot\cos(\theta)$$

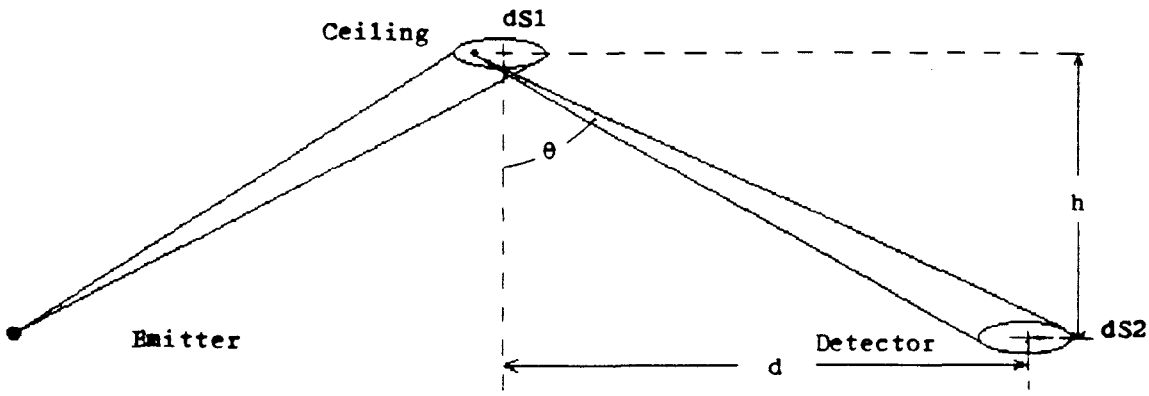

Figure 2.7
Small ceiling area's contribution
to floor radiant incidance

Where I is *radiant intensity* (watt per unit solid angle). It can be shown that $I(0)=\Phi/\pi$ for a half hemisphere diffuse radiator [2]. Therefore the radiant intensity viewed from dS_2 is

$$I(\theta) = \frac{d\Phi_1}{\pi}\cdot\cos(\theta)$$

The flux differential incident upon dS_2 is $I(\theta)$ times the solid angle formed by dS_2 and an imaginary point source at S_1:

$$d\Omega = \frac{dS_2}{d^2+h^2}\cdot\cos(\theta)$$

Therefore

$$d\Phi_2 = \frac{d\Phi_1}{\pi}\cdot\cos(\theta)\cdot\frac{dS_2}{d^2+h^2}\cdot\cos(\theta)$$

$$= \frac{1}{\pi}\cdot\frac{\cos^2(\theta)}{d^2+h^2}\cdot d\Phi_1\, d\Phi_2$$

The radiant incidance differential at dS_2 is $d\Phi_2/dS_2$:

$$dE_f = \frac{1}{\pi}\cdot\frac{\cos^2(\theta)}{d^2+h^2}\cdot d\Phi_1$$

Since $\cos^2(\theta)=h^2/(d^2+h^2)$,

$$dE_f = \frac{1}{\pi}\cdot\frac{h^2}{(d^2+h^2)^2}\cdot d\Phi_1$$

The exitant flux differential $d\Phi_1$ is the product of $M(\Phi,h,r,\mu)$ and dS_1:

$$dE_f = \frac{1}{\pi} \cdot \frac{h^2}{(d^2+h^2)^2} \cdot M_c(\Phi, h, r_1, \mu) \cdot dS_1 \qquad (2\text{-}3)$$

where r_1 is the horizontal distance from the emitting source to dS_1 (Figure 2.8).

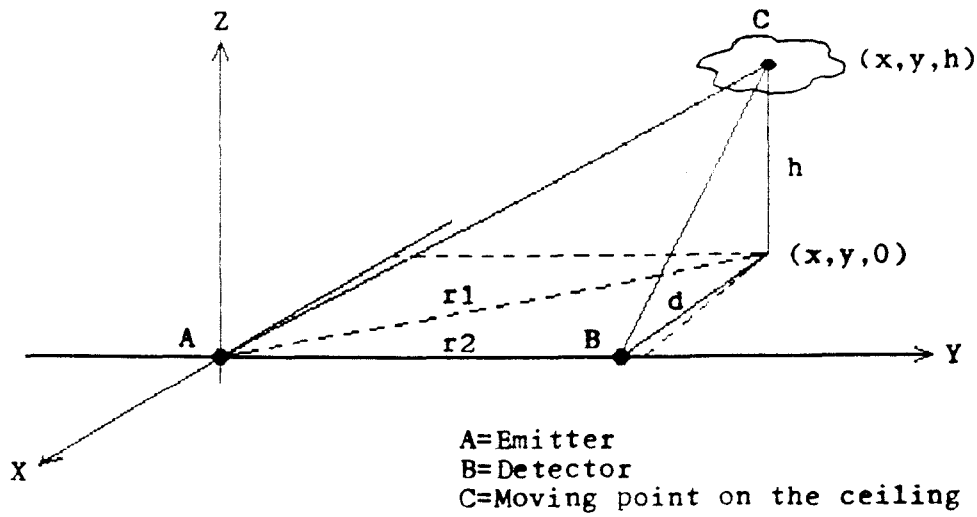

Figure 2.8
Geometric relation between the floor, ceiling, emitter and receiver

If point C is made the moving point for integration, its coordinate is (x,y,h). It is clear from Figure 2.7 and 2.8 that:

$$r_1^2 = x^2+y^2$$

$$d^2 = (x-r_2)^2+y^2$$

$$dS_1 = dxdy$$

Substituting (2-3) for $M_c(\Phi,h,r,\mu)$, r_1, d and dS_1 we obtain the differential form of the floor radiant incidance:

$$dE_f = \frac{\mu h^3 \Phi}{2\pi^2} \cdot \frac{1}{[(x-r_2)^2+y^2+h^2]^2} \cdot \frac{1}{[x^2+y^2+h^2]^{3/2}} \cdot dxdy \qquad (2\text{-}4)$$

The floor radiant incidance function is the integration of dE_f over the entire ceiling surface:

$$E_f(\Phi,h,r_2,\mu) = \frac{\mu h^3 \Phi}{2\pi^2} \int_{-\infty}^{\infty}\int \frac{1}{[(x-r_2)^2+y^2+h^2]^2} \cdot \frac{1}{[x^2+y^2+h^2]^{3/2}} \, dxdy$$

Figure 2.9 plots the floor illumination versus radius. Figure 2.10 plots the floor illumination over a floor plane. Since an analytic solution could not be found by the author, the above integral was numerically solved and plotted by a computer program.

The transmission efficiency for a ONP system can be determined from Figure 2.9 or 2.11 in which the curve of Figure 2.9 is magnified.

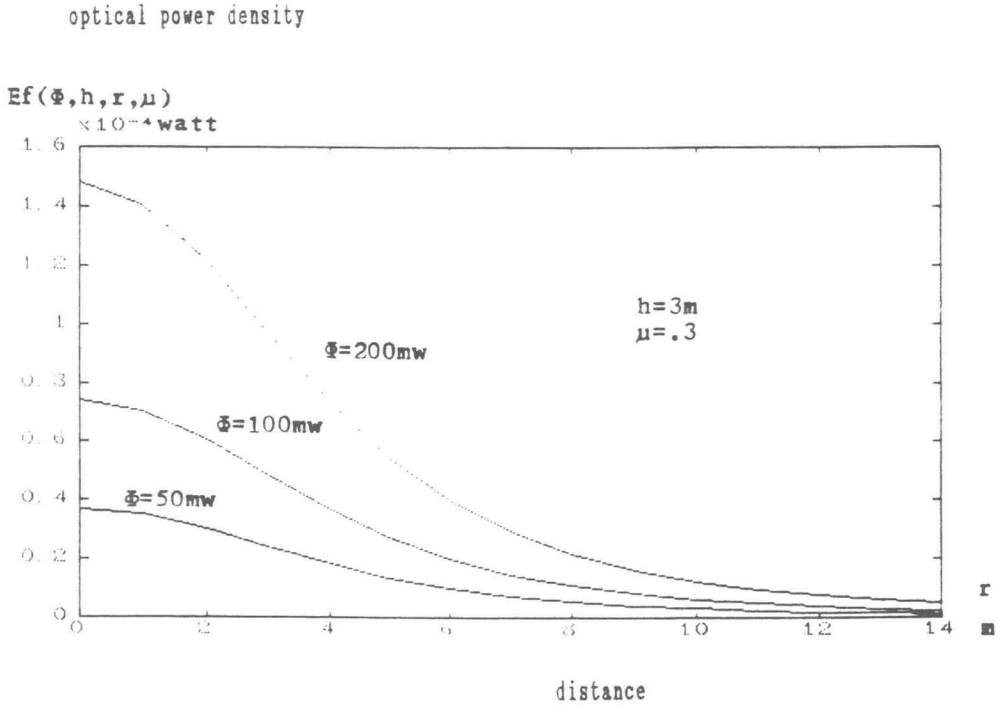

Figure 2.9

Floor incident power density as a function of distance between emitter and detector for omnidirectional and non-direct path optical communication system

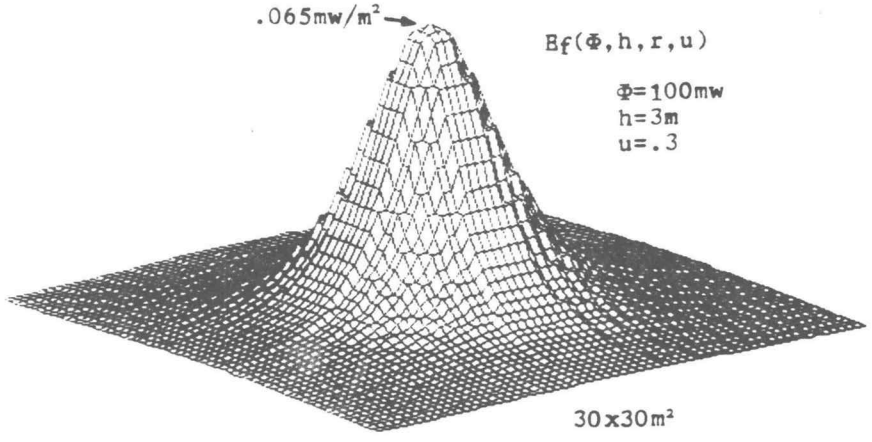

Figure 2.10

Floor incidant power density over a 30x30m² floor plane

Example 2.2

We use conditions similar to *Example 2.1* (distance=10 meters; effective photo detecting area diameter=2.5mm). The Φ=100mw curve shows that the floor illumination E_f is 0.62×10^{-5} watt/m^2 at 10 meters. The optical flux received by the detector (Φ_r) is the product of E_f and the effective detecting area:

$$\Phi_r = 0.62\times10^{-5}\times(\tfrac{1}{4}\pi\times0.0025^2)$$
$$= 0.304\times10^{-10} \text{ watt}$$

The optical transmission efficiency EFF is the ratio of received power to the total emitted power:

$$EFF_t = \frac{\Phi_r}{\Phi}$$
$$= \frac{0.304\times10^{-10}}{0.1}$$
$$= 0.304\times10^{-9}$$

This shows that the signal level in a ONP system is more than one thousand times weaker than in a FDP system at 10 meters.

2.3. Comparison of FDP and ONP Systems

The ONP system has many attractive characteristics that do not exist in the FDP system. Because it does not require line-of-sight, obstacles between the emitter and

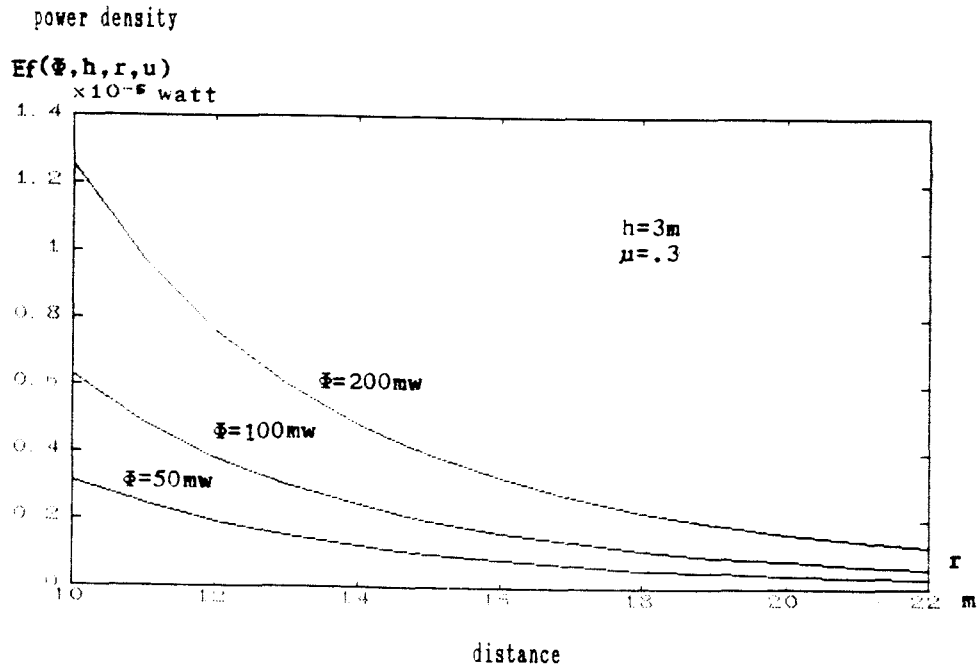

Figure 2.11

Magnified floor incident power density curve

the receiver do not affect communication as long as the light beams can reach the ceiling and walls which are line of sight to the receiver. The independence from orientation makes the system highly mobile within the room. Moreover, when a common carrier frequency channel is used, multiple units can be linked to form a multiple access local area network with the ceiling being the "bus".

Quantitative analysis in the previous sections shows that the signal power received by a photo detector in a ONP system may be several thousand times weaker than in a FDP system. This is a major obstacle in realizing a ONP system. Because of the stringent requirement of signal-to-noise ratio, complicated and systematically optimized system design approaches may be required.

CHAPTER THREE
ONP COMMUNICATION RANGE ESTIMATION

The optical signal power level in an ONP communication system may be several thousand times weaker than that of a conventional FDP system. It is impractical to raise the emitted optical power by thousands of times to obtain similar signal levels because of the limitations in cost and space. This raises the feasibility question for ONP systems. This problem will be discussed in this chapter. Criteria will be determined for the boundary of the communication range. The ONP communication range, as a function of total emitted power, data rate, and the noise figure of the photo detector, will be found.

The range of ONP communication covers a circular domain centered at the emitter. The electronic devices in a receiver generate internal noise signals. When the optical signal is sensed by the detector, the electric signal at the output of the detector is a mixture of the useful signal and the noise. For successful reception the signal level has to be large enough to be extracted from noise by the electronic circuits following the photo detector. As the distance increases, the useful signal level decreases and the SN ratio becomes smaller. At a certain radius the SN ratio is too small and is beyond the detection capability of the system. This radius is defined to be the communication range.

An ideal external communication channel is assumed. The ambient optical noise is ignored. The resulting range, therefore, is an upper bound value. For random signals and noise, unity (0dB) is usually considered the minimum SN ratio for successful signal recovery [7,10,12,13,14,15].

In the calculations that follow, a more conservative SN threshold of 2 will be used. This is expressed by

$$SN = P_e/P_n = 2 \qquad (3\text{-}1)$$

where P_e is the electrical signal power and P_n is the electrical noise power in the receiving device. the SN ratio in the photo detector is dominant and determines the receiver's overall SN ratio, because it is the first stage of the receiver, and the noise power in a photo detector is much higher than that in a transistor [5].

P_e in a photo detector can be calculated knowing the floor illumination function E_f, the effective detecting area S and the optical filter transmission ratio η of the photo detector:

$$P_e = \eta \cdot E_f(\Phi,h,r,\mu) \cdot S$$

The noise power in a photo detector is usually characterized by NEP, the "noise equivalent power". NEP is the incident radiant signal power needed for unity signal-to-noise ratio, and is normalized to bandwidth. It has units of watt/$\sqrt{Hz}$. For a high efficiency PIN photo detector (see Appendix B), NEP is typically 4.2×10^{-10} watt/$\sqrt{Hz}$. It can be seen that the noise power is also related to the desired frequency bandwidth. For a specified SN ratio the incident radiant signal power threshold can be calculated as follows:

$$P_e = SN \cdot NEP \cdot \sqrt{BW}$$

where BW is the signal bandwidth. SN can then be written as follows:

$$SN = \frac{\eta \cdot E_f(\Phi,h,r,\mu) \cdot S}{NEP \cdot \sqrt{BW}} \qquad (3\text{-}2)$$

As can be seen from the above equation, both Φ and r are expressed in implicit form. Their values must be found to determine the feasibility of the communication system. As there is no known analytical solution to the illumination function, numerical computations are required to evaluate r or Φ with all other variables known. Since the illumination function is a linear function of Φ (therefore it is proportional to the SN ratio), it is easier to find the required total emitted power given r rather than vice versa.

Example: 3.1

Assume that an ONP optical communication system has the following parameters:

Communication range: r=10m
Distance from devices to ceiling: h=3m
Reflectant ratio: μ=0.3
Photo detector effective detecting area: S=5mm^2
Photo detector optical efficiency: η=0.5
Photo detector noise: NEP=4.2x10^{-14}w/$\sqrt{Hz}$
Signal bandwidth: BW=5kHz

To utilize the illumination function curve of Figure 2.9 and Figure 2.11, we choose Φ=K$\cdot$100mw and use the property of linearity $E_f(K\cdot\Phi,h,r,\mu)= K\cdot E_f(\Phi,h,r,\mu)$:

$$SN = \frac{\eta \cdot S \cdot K \cdot E_f(0.1,h,r,\mu)}{NEP \cdot \sqrt{BW}}$$

K can be calculated by letting SN=2:

$$K = \frac{SN \cdot NEP \cdot \sqrt{BW}}{\eta \cdot S \cdot E_f(0.1,h,r,\mu)}$$

$$= \frac{2\times4.2\times10^{-14}\times\sqrt{5000}}{0.5\times5\times10^{-6}\times E_f(0.1,3,10,0.3)}$$

From Figure 2.11, $E_f(0.1,3,10,0.3)=0.62\times10^{-5}$. The value of K is found to be 0.383. The total emitted power required is then $\Phi=K\cdot100mw=0.383\times100=38.3mw$. Since the other parameters used in this estimation are typical, this result states that for a lossless communication channel, the ONP communication radius can be 10 meters with only 38.3mw emitted optical power. In actual systems, modulation is almost certainly used. This results in at least several dB loss in SN ratio. Assuming a 5dB loss in communication channel, the 10 meter range can be achieved with 121mw of optical power.

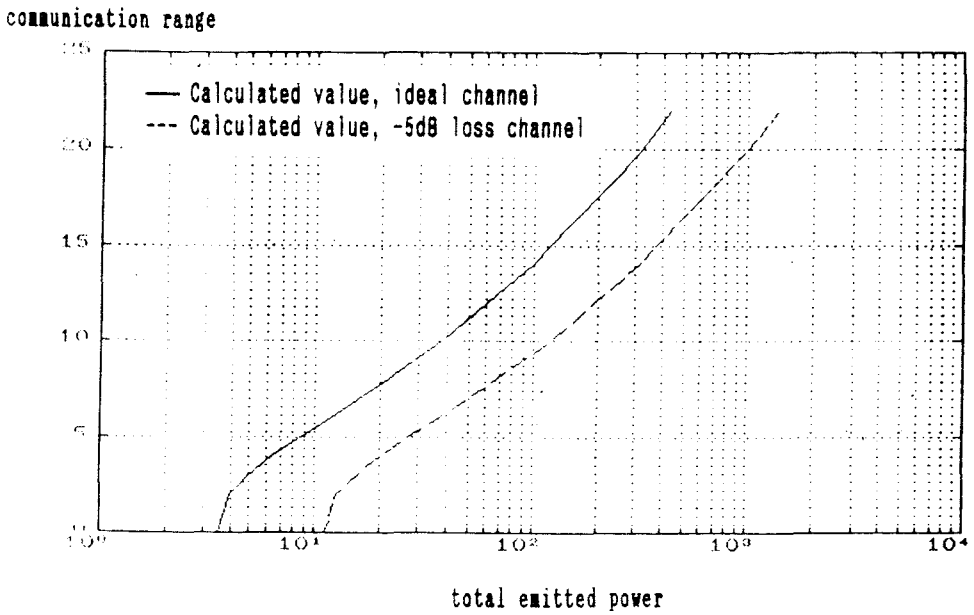

Figure 3.1

Plot of communication range vs optical power

(other parameters similar to *Example 3.1*)

Most rooms are smaller than a circle of 20 meters in diameter. 121mw optical power can be obtained by a few infrared LEDs. The conclusion here is that the idea of the ONP system is feasible.

Figure 3.1 plots the ONP communication range versus required total optical power. The solid line is for an ideal communication channel and the dashed line is for a communication channel with 5dB loss in SN ratio. All other parameters are similar to *Example 3.1*.

Although the analytic solution can not be found, some simple function can be sought to approximate the range-power curve shown by Figure 3.1. One such function has been found as follows.

Since most part of the curve is roughly a straight line and the curve is plotted in semilog scale, the curve is first approximated by

$$R = k_1 \cdot \log_{10} P + k_2$$

where k_1 and k_2 are constants. $k_1 \cdot \log_{10} P$ is then replaced by $k \cdot \log P + k_2$. The function can then be equivalently expressed by

$$P = k' e^{R/k},$$

where k and k' are constants. Ignoring the curly portion of the curve at small values of R, the main portion of the curves can be approximated with k'=2.5 and k=4 for the ideal channel, k'=7.9 and k=4 for the 5dB loss channel, respectively. Figure 3.2 shows the approximated analytical solution for the power-range relationship.

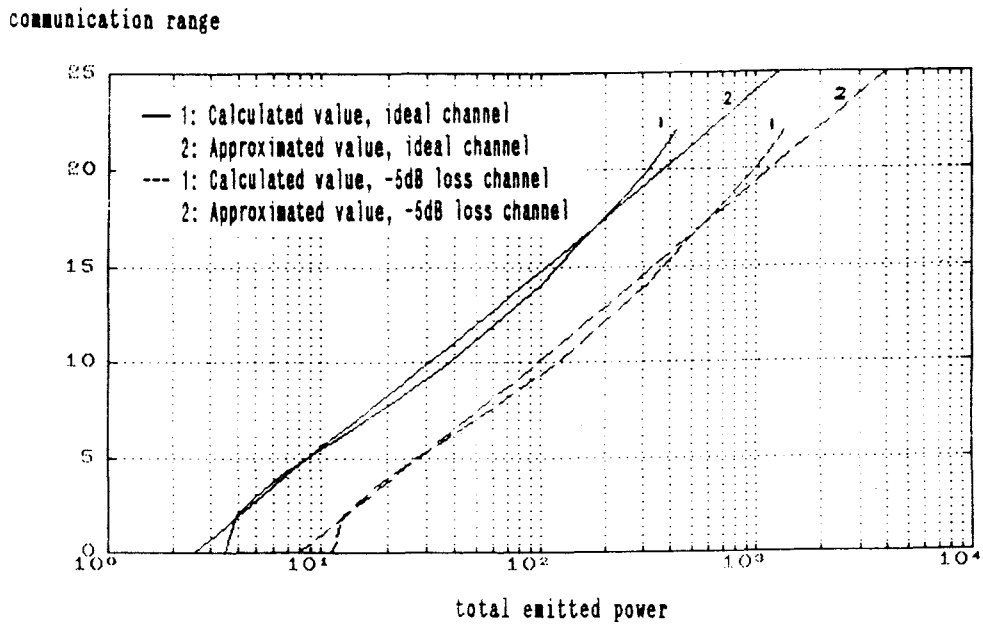

Figure 3.2
Plot of approximated analytical solution for
the communication range versus optical power

The approximated analytical solution shows that the required optical power is an exponential function of the range. The required optical power increases rapidly with increased range. In other words, ONP systems become impractical for larger ranges due to the required high level of optical power.

CHAPTER FOUR

EFFICIENCY ANALYSIS FOR MODULATED LED TRANSMITTER

In this chapter rules are developed that will lead to maximum efficiency for a LED optical communication transmitter that employs a modulated carrier frequency. The use of modulation techniques in a noisy communication condition has been proven to effectively raise the system's overall performance. This will be addressed later in Chapter Five.

The normalized performance index (NPI) of a LED optical communication transmitter is defined as the value of a performance index per unit of electrical power consumed by the LED's. Since any LED has a limit of power dissipation, the total consumed power is proportional to the number of LED's used. Therefore, the NPI can also be interpreted as the performance index obtainable from a single LED. There can be many definitions of NPI. For instance, when communication range is of interest, we like to maximize the useful output light power obtainable per unit of consumed power. When we are interested in data rate as well as range, we may choose the product of range and data rate obtainable per unit consumed power as the NPI.

This chapter systematically analyses the transmitter performance index using a linearized LED model. The LED driver is assumed to work in a switching mode, that is, the driving current has an "on" level and an "off" (or zero) level. The power output of interest is the first harmonic of the output optical signal, since most

receivers employ a tuned front-end filter to receive the main lobe of the signal spectrum. Therefore, the normalized performance index is the ratio of the first harmonic output optical signal power to the electrical power required to drive the LED.

On the basis of the analysis, a set of rules is established in graphical and analytical form that can be used as design tools to achieve best transmitter performance under various conditions.

4.1 The Model for an Infrared LED

An infrared LED is a current controlled optical power source. It presents good linearity in the usable current range. Figure 4.1a shows the emitted power vs driving current for a typical infrared LED.

The terminal characteristics of an LED are very similar to those of a silicon diode, with the junction voltage drop being higher. Figure 4.1b illustrates the I-V curve of a typical infrared LED. When calculating the electrical power consumed by a LED, the terminal voltage can be assumed to be constant, hence the average electrical power is proportional to the average driving current.

Figure 4.2 illustrates the transient response of a typical infrared LED. When the driving current is turned on and off, the output optical power resembles exponential curves. The delays for the "on" and "off" current transitions are measured by the rise time t_r and fall time t_f, respectively.

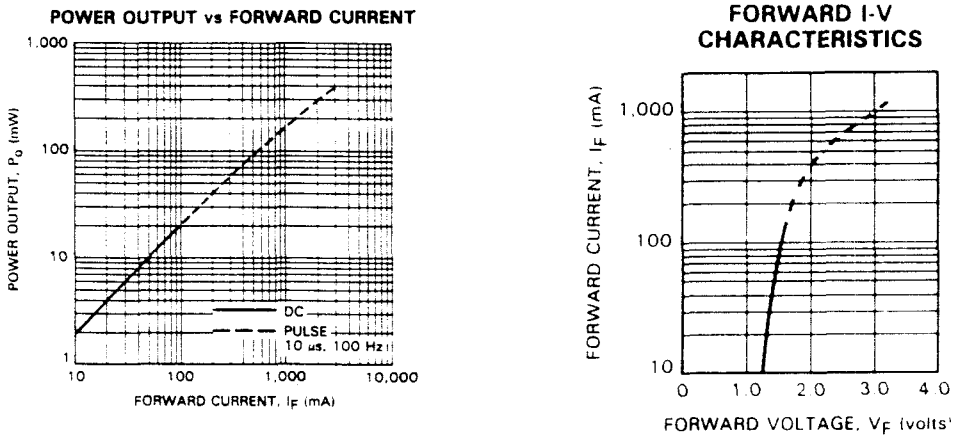

Figure 4.1
Infrared LED's static characteristics [11]

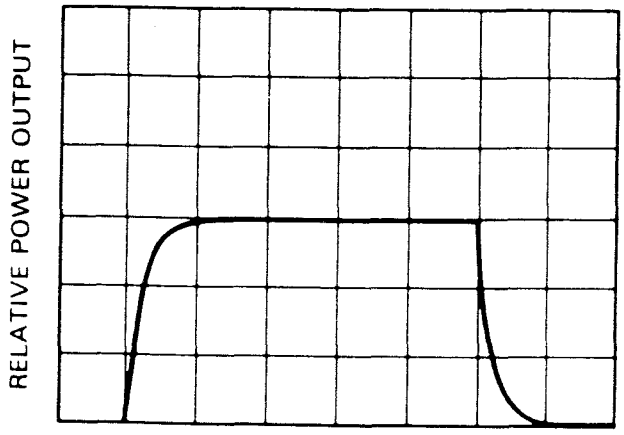

Figure 4.2
Infrared LED's transient characteristics [11]

To simplify the calculation in the Fourier series analysis that will follow shortly, we now establish a model for the LED. The model has the following characteristics:

1) The power transfer function is linear

2) The power output response to a step current input is a ramp function before it reaches the steady state.

The slope of the ramp is determined in the following way: the optical energy generated by the real and modeled LED are the same. In Figure 4.3, this requires the areas under the solid curve and the dotted curve be the same. The dotted curve can be described by $1-e^{-t/T}$ where T is a constant. Let the time integral of the two curves be the same:

$$\lim_{t->\infty}[\tfrac{1}{2}t_s+(t-t_s) - \int_{\delta=0}^{t}(1-e^{-\delta/T})d\delta] = 0$$

or

$$\lim_{t->\infty}[T(e^{-t/T}-1)+\tfrac{1}{2}t_s] = 0$$

or

$$t_s = 2T \qquad (4-1)$$

Since the response time of an infrared LED is usually given in the form of rise time (t_r) and fall time (t_f) instead of the time constant T of the exponential curve, we need to translate t_r and t_f into T_r and T_f so that the ramp time (switching time) t_s can be expressed in terms of t_r or t_f. Both t_r and t_f are defined as the time needed for the quantity to change from the 10% point to the 90% point, as shown by Figure 4.3.

The relationship between T_r and t_r is found by solving the exponential curve for T_r at t_r values 0.1 and 0.9:

$$T_r = t_r/2.2$$

The same relation holds between t_f and T_f. Replacing T in (4-1) we obtain the relation between the model's ramp time and LED's rise and fall time:

$$t_{sr} = 0.91t_r$$
$$t_{sf} = 0.91t_f$$

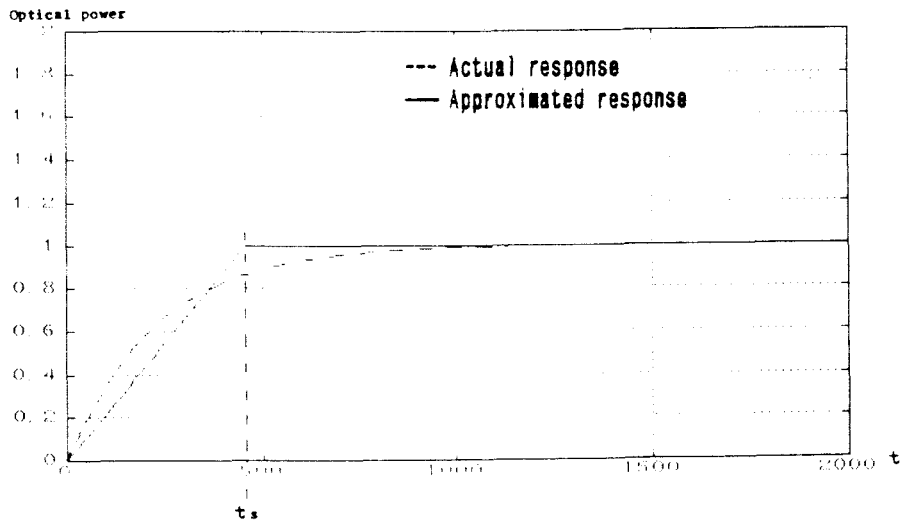

Figure 4.3
Approximated step response of LED

At larger driving current, the infrared LED's rise time and fall time approach the same value, as illustrated by Figure 4.4. In switching mode operations, the LED is commonly driven by large current for higher device utilization. Therefore the same ramp time will be used for both the rising and falling period, denoted by t_s, the switching time of the output optical power. It can be calculated by $t_s = 0.91t_r$. The model of the infrared LED is then completed, as illustrated by Figure 4.5.

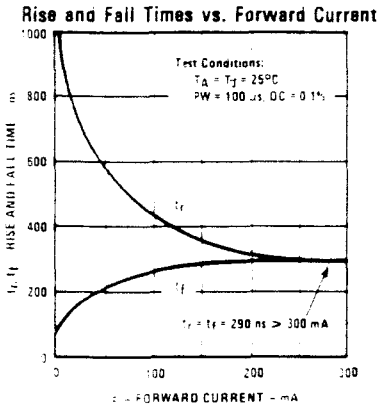

Figure 4.4
Rise and fall time of a LED

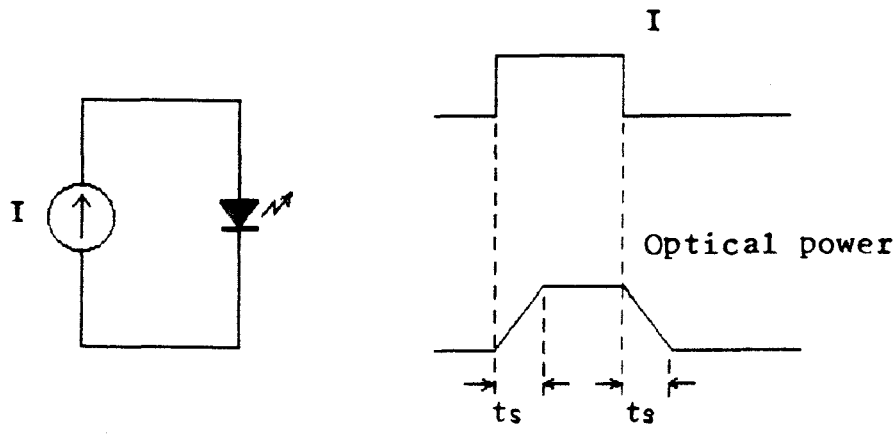

Figure 4.5
The model of an infrared LED

4.2 The LED Driving Method

Two important parameters are now defined which completely specify how the LED model is driven by a periodical on-off type input current function.

Switching time duty cycle α. α is the ratio of the LED's switching time t_s to the period of the driving current. Since $\alpha = f \cdot t_s = f/t_s^{-1}$, it is also the carrier frequency normalized to 1/ts.

Driving current duty cycle β. β is the ratio of the "on" time to the period of the driving current.

These are illustrated by Figure 4.6. For convenience the frequency and amplitude of the driving current is normalized. Since the optical power efficiency is based

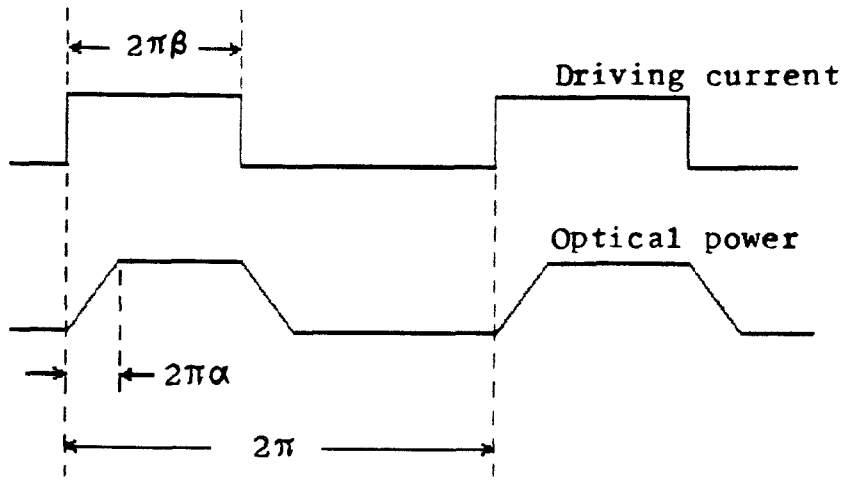

Figure 4.6
Relationship between switching cycle (α) and driving current duty cycle (β) for a LED.

on time average, the normalization will not affect the results. All the math manipulations that follow are linear so the amplitude normalization can be easily restored when needed.

When the LED switching time is fixed, α is proportional to the driving frequency. Therefore, α and β define the frequency and duty cycle of the driving current. These two parameters are exactly what a system designer needs to know.

Both α and β affect the output optical power in terms of its first harmonic, the power component useful to a receiver. As α (or frequency) increases, more driving power is wasted in the switching period, causing the optical power efficiency to decrease which results in a shorter communication range. Increased carrier frequency, on the other hand, can carry more information per unit time. As β decreases, both output power and the driving power decrease. There is apparently a trade-off between the power efficiency and data rate. Only quantitative analysis can help a designer to choose α and β to meet his particularly weighted interests in optical power efficiency and data rate.

4.3 Power Efficiency as a Function of α and β

We have defined the optical power efficiency earlier as the ratio of the useful (or first harmonic) output optical power emitted from a infrared LED to the electrical power consumed by the LED. Our interest here is

to find the conditions (α and β) leading to the maximum useful output optical power efficiency.

Since the LED has a nearly constant terminal voltage for a large range of driving current, the electrical power consumed by the LED can be considered to be proportional to the average of the driving current. The average driving current is proportional to β, so the electrical power consumption is also proportional to β.

The first harmonic of the output optical power is determined by the shape of the optical output power waveform, hence it is a function of both α and β. The first harmonic of the waveform can be determined from the Fourier series analysis. Figure 4.7 shows the two possible cases of the output optical power waveform.

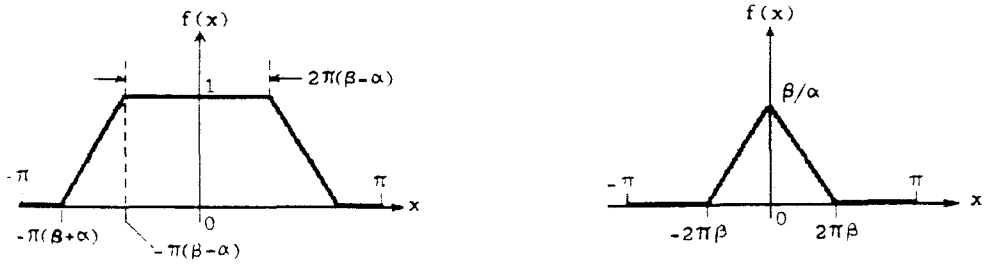

case 1 β≥α case 2 β<α

Figure 4.7
Output optical power waveforms

The optical power function can be described by the following equations:

if $\beta \geq \alpha$ (case 1)

$$f(x) = \begin{cases} 0 & x \in [-\pi, -\pi(\beta+\alpha)) \\ \frac{1}{2\pi\alpha} \cdot [x+\pi(\beta+\alpha)] & x \in [-\pi(\beta+\alpha), -\pi(\beta-\alpha)) \\ 1 & x \in [-\pi(\beta-\alpha), 0] \end{cases}$$

if $\beta < \alpha$ (case 2)

$$f(x) = \begin{cases} 0 & x \in [-\pi, -2\pi\beta) \\ \frac{1}{2\pi\alpha} \cdot (x+2\pi\beta) & x \in [-2\pi\beta, 0) \end{cases}$$

and $f(-x)=f(x)$. The functions are symetric about x=0. The Fourier series is

$$f(x) = \frac{a_0}{2} + \sum_{n=1}^{\infty} [a_n \cos(nx)+b_n \sin(nx)] \qquad (4\text{-}2)$$

The function is symetric about x=0, therefore all b_n are zero. We are interested in finding $a_1 = f(x)\big|_{n=1}$ only:

$$a_1 = \frac{1}{\pi} \cdot \int_{-\pi}^{\pi} f(x) \cdot \cos(x) \cdot dx$$

$$= \frac{2}{\pi} \cdot \int_{-\pi}^{0} f(x) \cdot \cos(x) \cdot dx$$

The solution is found as

$$a_1 = \begin{cases} \frac{2}{\alpha\pi^2} \cdot \sin(\pi\beta) \cdot \sin(\pi\alpha) & \beta \geq \alpha \\ \frac{1}{\alpha\pi^2} \cdot [1-\cos(2\pi\beta)] & \beta < \alpha \end{cases} \qquad (4\text{-}3)$$

The series is convergent because f(x) satisfies Dirichlet's sufficient condition for convergence (piecewise smooth), as illustrated by Figure 4.7.

(4-3) represents the useful output optical power as a function of normalized carrier frequency and driving current duty cycle. It is plotted in Figure 4.8. It indicates that, to obtain maximum useful optical power without considering efficiency, β should be 0.5 (square wave driving current with 50% duty cycle) and a low carrier frequency should be used.

Dividing a_1 by β, which is proportional to power consumption, we get the optical power efficiency function $E_p(\alpha,\beta)$ of Figure 4.9.

Figure 4.10 is the same function with several emphasizing curves, dividing the surface into several zones. Line ABE is the line with $\alpha=\beta$. Line ABF is the maximum efficiency line for specified α's. Two important conclusions can be drawn from the power efficiency surface:

1) Given the normalized carrier frequency (or α), there exists an optimal driving current duty cycle. The value of this optimal β is equal to α if α is less than 0.371, and is equal to 0.371 otherwise;

2) Smaller α (or lower frequency) yields higher power efficiency. Lower frequencies should be used whenever possible, if the optical power efficiency is to be maximized.

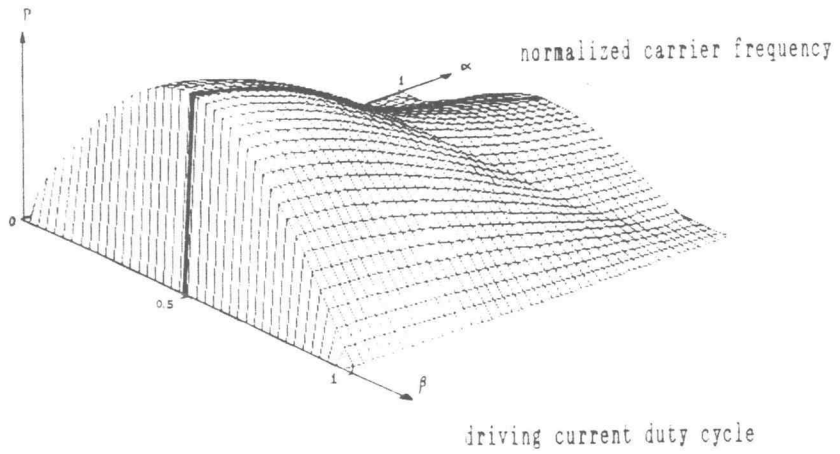

Figure 4.8

Output optical power as a function of normalized carrier frequency and driving current duty cycle.

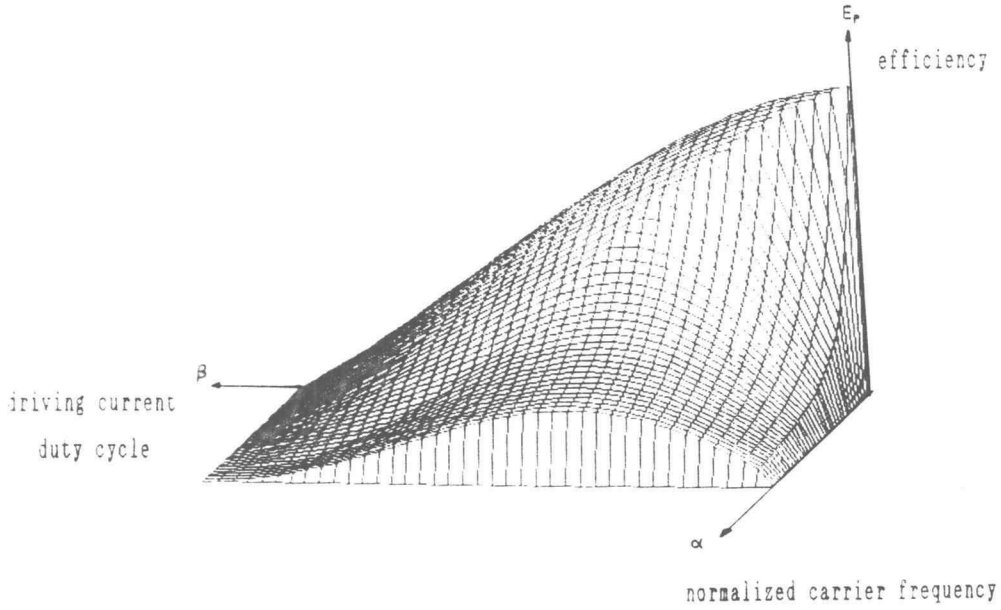

Figure 4.9

Power efficiency as a function of normalized carrier frequency and driving current duty cycle.

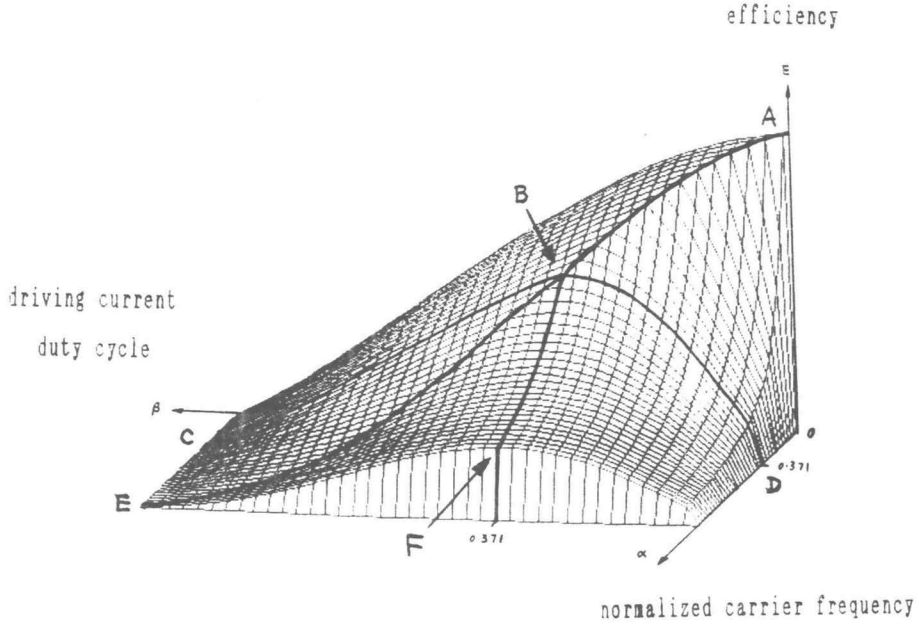

Figure 4.10

Power efficiency function

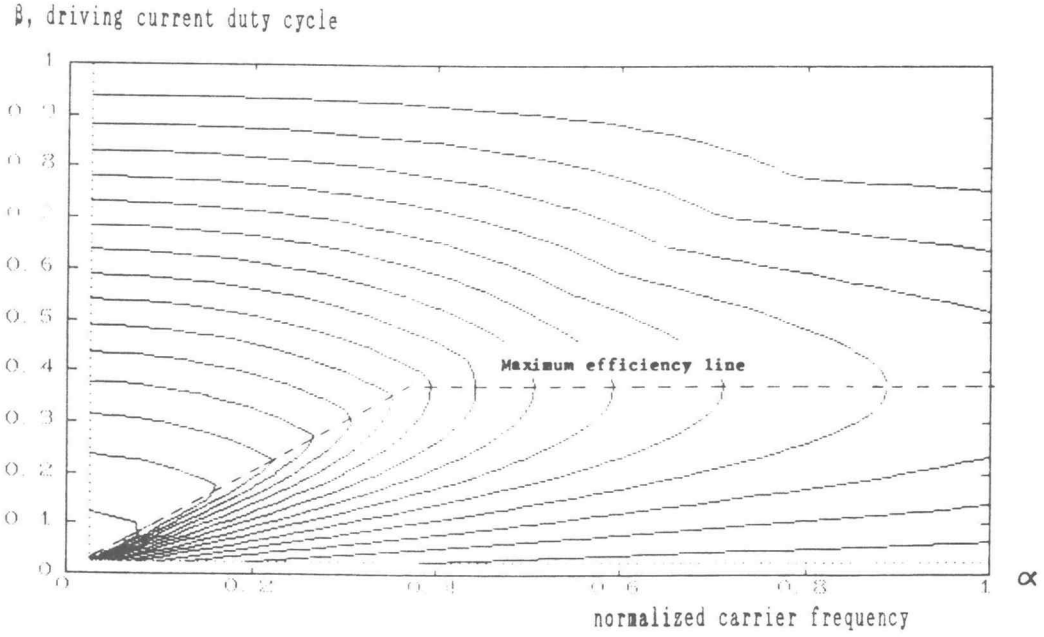

Figure 4.11

Power efficiency function contour

Considering the above facts, the suitable working point of the LED driver should be chosen along line AB in Figure 4.10. It is interesting to note that the best efficiencies are obtained when the output optical power waveform is a triangle pulse train (since $\alpha \geq \beta$ along ABF). Figure 4.10 plots the contour of the efficiency curve for higher readability.

The significance of the power efficiency function is that it provides an easy way for designers to select a proper carrier frequency and an optimal driving current duty cycle to achieve maximum optical power efficiency, or in other words, to use the least amount of power and smallest number of devices.

Example 4.1

Assume that the center carrier frequency f_o of a modulated infrared data communication system is limited within 100 kHz to 500 kHz. The Infrared LED selected has a rise/fall time t_r of 0.5μs. Determine the proper carrier frequency and driving current duty cycle.

Solution:

From Figure 4.10 we know that a smaller α results in a higher efficiency. Since α is proportional to f_o, we choose f_o=100kHz. α can be calculated by its definition:

$$\alpha = \frac{\text{LED switching time}}{\text{Driving current cycle}}$$

$$= 0.91 \cdot t_r \cdot f_o$$

$$= 0.91 \times 0.5 \times 10^{-6} \times 500 \times 10^{3}$$

$$= 0.046$$

β can then be determined from Figure 4.10. Since α is less than 0.371, the point is on line AB of Figure 4.10 and β is the same as α (0.046). The actual value of β should be slightly greater than 0.046 to tolerate error so that the curve would not go into the sharply dropping zone of $\beta < \alpha$.

4.4 Comprehensive Optimization

The previous section solved the problem of finding the optimal duty cycle. The "optimal" carrier frequency (or α), however, does not exist in general, since the definition of optimal frequency might be different in different situations.

Generally, the carrier frequency affects the power efficiency and the data rate in opposite ways. On the one hand, a lower carrier frequency yields higher power efficiency because less power is wasted in switching the LED (Figure 4.9). On the other hand, a higher carrier frequency shifts the signal band farther from the ambient noise spectrum, and often makes the receiver's front-end filter more efficient. If the frequency were to be optimized, there has to be a comprehensive performance index (or "figure of merit") that combines the power efficiency and data rate in some way. In the example that follows, we illustrate how a transmitter is optimized toward a particular performance index with an illustrative ambient noise power density spectrum.

Example 4.2

An ONP infrared data communication system uses FM modulation techniques. The area of the transmission domain of the transmitter is considered equally important to the communication data rate. The ambient infrared noise power has its highest density in the lower frequency band. For example, assume that the spectral density is described by $N=(10\alpha+1)/(\alpha+10)$ where α is the normalized frequency. The LED has a rise/fall time of 0.5 μs. Determine an optimal set of carrier frequency and driving current duty cycle.

Solution:

Since the communication area and data rate are equally important, we use the product of the two divided by the power consumption as the performance index to judge the optimization. This choice gives the communication area and the data rate the same effect in affecting the index.

It can be seen from the illumination functions in Chapter Two that the floor illumination level is roughly inversely proportional to Φ/r^2 (P_o/r^2 in this case). Range r is roughly proportional to $\sqrt{P_o}$, so the area covered by the communication is roughly proportional to P_o. For a FM receiver having a certain modulation index, the channel capacity (proportional to the maximum data rate) is inversely proportional to the noise power spectral density [10], [13]. Therefore the performance index can be chosen as

$$Q = n^{-1} \cdot P_o/P_e$$

$$= n^{-1} \cdot E_p(\alpha,\beta)$$

$$= \frac{\alpha+10}{10\alpha+1} \cdot a_1/\beta$$

where α is the carrier frequency normalized to the LED's switching frequency $1/t_s$; a_1 is the first harmonic of the output optical power expressed by Eq. (4-3).

Q can be conveniently evaluated by a computer program. Figure 4.12 illustrates the numerical solution to Q near its peak point. Q is also plotted in Figure 4.13, and its contour is plotted in Figure 4.14 for accurate reading.

Now the carrier frequency and driving current duty cycle can be calculated:

$$f_o = \frac{\alpha}{t_s}$$

$$= \frac{\alpha}{0.91 \cdot t_r}$$

$$= \frac{0.308}{0.91 \times 0.5 \times 10^{-6}}$$

$$= 677 \text{ kHz}$$

and β=0.308 from Figure 4.14. Therefore the system should use a center carrier frequency of about 677 kHz and a driving current duty cycle of 30.8% for highest efficiency in terms of communication covered area and data rate.

α	β	Q
.3060	.3060	.660710
.3065	.3065	.660719
.3070	.3070	.660725
.3075	.3075	.660728
.3080	**.3080**	**.660729**
.3085	.3085	.660727
.3090	.3090	.660723
.3095	.3095	.660717
.3100	.3100	.660708

Figure 4.12

Maximum Q (Q_{max} is printed in boldface)

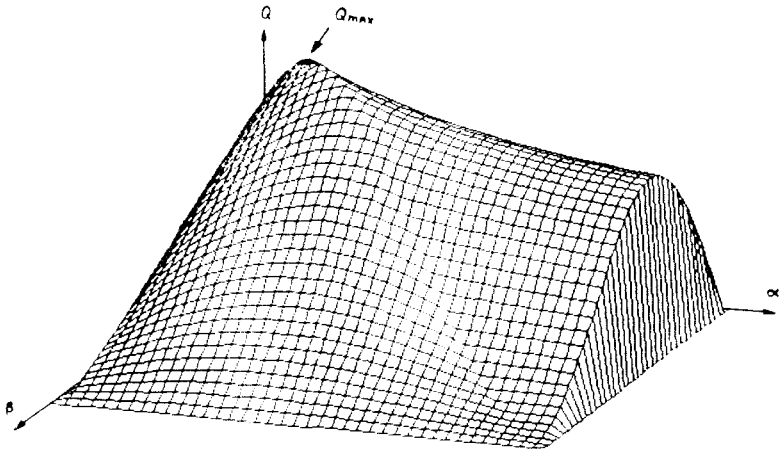

Figure 4.13

Comprehensive optimization index Q(α,β)

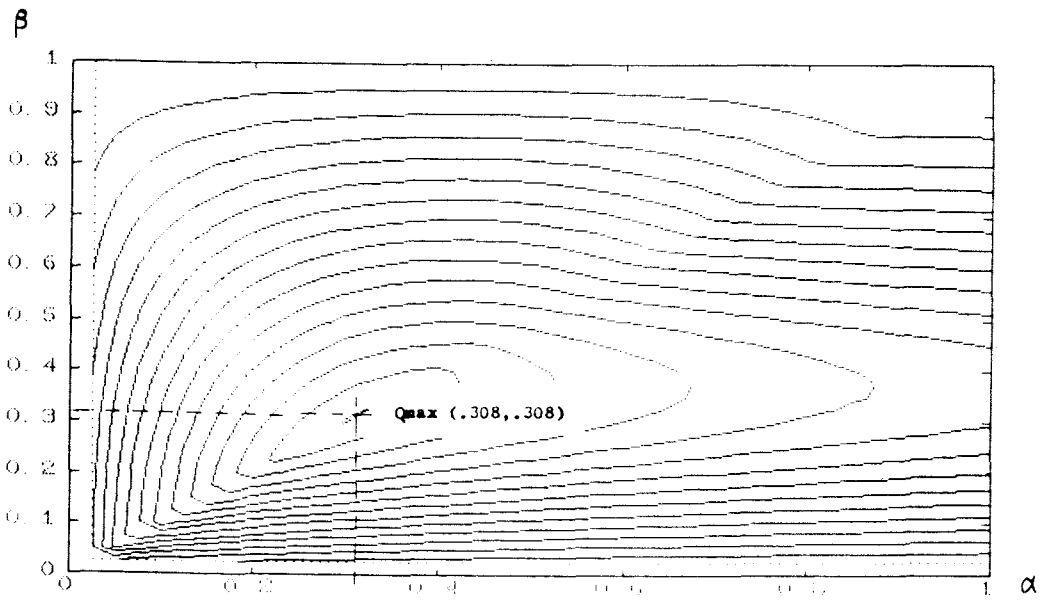

Figure 4.14
Contour of Q(α,β)

CHAPTER FIVE

OMNIDIRECTIONAL AND NON-DIRECT PATH OPTICAL COMMUNICATION EXPERIMENTS

On the basis of the analysis done in the previous chapters, the author has experimented in designing and implementing a ONP infrared optical data communication system (named OptoNet). In this chapter, the process of design will be illustrated and the test results, which have been successful, will be presented.

The results of the experiments not only support the theoretical analysis but also showed that infrared light generated by LEDs can successfully be used to implement omnidirectional and non-direct path indoor data communications.

The experiment was designed to determine the following characteristics:

1. Range vs Transmitter Orientation;
2. Range vs Receiver Orientation;
3. Range vs optical power;
4. Error rate vs distance.

5.1 System Level Considerations

The system consists of two identical communication units. Each contains an infrared light transmitter, an infrared light receiver, and the required control hardware and software. The two units were placed in arbitrary

locations far apart from each other in a large room. A workbench was used as the barrier which blocked the line-of-sight between the units. Optical signals traveled between the two units via reflection off the ceiling.

The most fundamental design consideration is to select the frequency spectrum band in which the data is to be contained. In its simplest form the data can be represented by the emitted optical power level; A "one" turns on the optical emitter and a "0" turns it off. This is sometimes called "base band" transmission since the frequency spectrum of the transmitted signal is the same as that of the data. If a higher frequency is used as the carrier which is modulated by the data, the signal is usually shifted to a higher frequency band. This is called "broad band" transmission.

Whether or not modulation is needed depends upon such factors as the ambient noise spectrum, transmission efficiency, frequency usage regulations, etc [14]. In our case, the major concern is to minimize the ambient noise interference.

The minimum amount of signal power to be received by the photo detector is in the vicinity of the level of the internal noise power in the detector [14,15]. In reality, the photo-detector sees not only the signal but also the ambient or "noise" light. This is the sum of infrared power from sources like solar illumination, interior lighting, light from a computer monitor, a TV remote controller, etc. Most energy in these noise sources is concentrated at a constant d.c. and lower frequency range.

An illustrative plot of the indoor ambient light energy spectrum, as seen by a 880nm photo detector, is

shown in Figure 5.1 [16]. The smaller lobes at multiples of 60Hz are due to the 60Hz electricity powering the lamps in the room. These lobes attenuate very quickly with increasing frequency due to the low speed response of the lighting materials used in the lamps, mainly the incandescent lamp and the flourescent lamps. There is also a wideband white noise background that is generated by all sources generating near infrared energy.

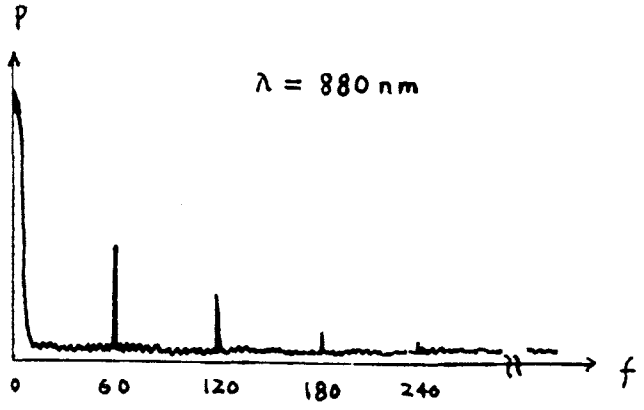

Fig 5.1
Noise spectrum of indoor ambient IR light

The spectrum of most forms of data occupies the range from d.c. up to a certain frequency. The ambient light spectrum overlaps with the data's spectrum and could override data by thousands of times in power level. It is therefore mandatory for near infrared optical communication system to use broadband technology to eliminate the unwanted noise signal of ambient light. Since the ambient noise energy is concentrated below several kilohertz, the carrier frequency of the broad band

signal should be at least several tens of kilohertz.

The choice of a modulation scheme is another important decision to make. Modulation theory and practice are discussed in detail in the literature and will not be dealt with here. It is well known that FM modulation is superior in overcoming noise. When the modulating signal is of discrete nature, the FM modulation is also called FSK or frequency shift keying. Two level FSK is used in the experimental system for its simple implementation.

5.2. Transmitter Design

The major parameters to be determined are the carrier frequency, driving current duty cycle, driving current amplitude and modulation parameters.

The carrier frequency used in the experiment has been chosen mainly according to component availability. The radio IF frequency (a 455 kHz frequency internal to RF receivers) has been chosen because filters are readily available at this frequency band. 455 kHz is far enough from the low interference IR spectrum yet can be still handled by IR LEDs. The center carrier frequency used is 445 kHz which is conveniently derived from the system clock frequency and is still within the tuning range of the standard 455 kHz components.

The normalized frequency α was found as 0.202 (refer to *Example 4.1*). The driving current duty cycle β can then be determined using the curve in Figure 4.10. For the typical GaAlAs infrared LED used in the experimental system, the optimal duty cycle has been found as 0.202. In the actual implementation, however, a greater β value of

0.4 has been used, merely for the simplicity of hardware, since a single CMOS counter could be used both as a duty cycle controller and frequency synthesizer. This has resulted in a system with lower power efficiency (roughly 10% loss in efficiency, as can be evaluated by using Figure 4.10 and 4.11).

The first harmonic component in the output optical power of a LED can be calculated as follows. First, find k, the d.c. power transfer ratio of the LED from the data sheet (it is 0.2mW/mA for the LEDs used in OptoNet). The peak of the output pulse is then the on-state driving current times this ratio. Equation (4-3) can then be used to evaluate the peak of first harmonic component. The average first harmonic (or sine wave) power is obtained by multiplying the peak value by $2/\pi$. In the OptoNet experiment, $\alpha=0.202$ and $\beta=0.4$. Designating the on-state driving current as I_{on}, the first harmonic component of the output optical power is:

$$P = k\cdot\frac{2}{\alpha\pi^2}\cdot\sin(\pi\beta)\cdot\sin(\pi\alpha)\cdot\frac{2}{\pi}I_{on}$$

$$= 0.072\cdot I_{on} \qquad (mW)$$

I_{on} in the expression has the unit of mA.

The LED driver was designed such that by changing the value of two resistors the on-state driving current can be altered. This provided an easy way of measuring the curve of range vs optical power.

The modulation deviation is ±3.7% as a result of using a modulo 13-14 variable divider in the frequency synthesis. With a data rate of several kilohertz this deviation makes the system work as a wideband FM system,

which has a detection threshold of 5 dB at unity input SN ratio and a good output SN ratio for larger input SN ratios[14,15]. The bandwidth occupied by the FM signal can be roughly calculated by BW=2B+2F, where B is the useful bandwidth of the data, F is the frequency deviation and is equal to the center frequency times the modulation deviation [14]. The block diagram of the transmitter is shown in Figure 5.3.

5.3 Receiver Design

The receiver is quite similar to a FM radio communication receiver with the RF front-end and mixer replaced by an IR front end. The key design considerations are the input network and the total system gain.

The "antenna" of an IR receiver is the four photo diodes which convert optical power into corresponding electrical current. The four PIN photodiodes are physically placed in a hemisphere arrangement, pointing in four directions. Unlike a RF antenna, which usually has a low impedance of 50 ohms, photodiodes are current source type devices and have very high impedances in the vicinity of 100k ohm. The equivalent circuit of a photodoide is shown by Figure 5.3. The capacitance is caused by the PN junction capacitance.

To efficiently draw signal power from the photodiodes a JFET transistor is used. Its high input impedance not only matches the photodiodes but also makes filter coupling easier. A double-tuned LC network is used for the front-end filter. It is designed to have a flat response from 420 to 470 kHz to include the FM signal with a data rate up to 5000 bit/sec.

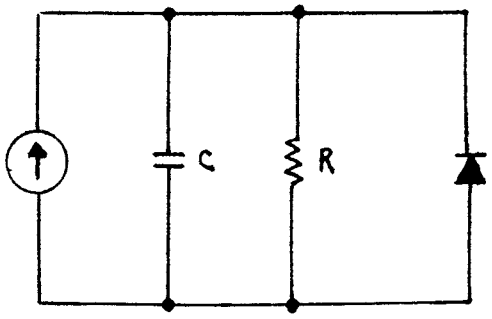

Fig 5.2
Equivalent circuit of photo diodes

An FM limiter/demodulator IC MC3361 is used as the main amplifier. The MC3361 works well with an input voltage of 1mv applied to its 1k input resistance. This requires an input power of 10^{-9} watt. A front-end amplifier is needed to boost the photodiode signal to at least this level. The smallest meaningful signal from the photodiode is around NEP*$\sqrt{B}$:

$$NEP*\sqrt{B}=4.2*10^{-14}*\sqrt{5000}=3*10^{-12}\ (watt)$$

The gain needed is then

$$10^{-9}/3*10^{-12}=25dB$$

Consider the 5dB detection threshold of the FM system, the minimum gain required for the front-end is 20dB. This is implemented by a two transistor amplifier stage, providing more than 30 dB gain at 445 kHz. The block diagram of the receiver is shown in Figure 5.3.

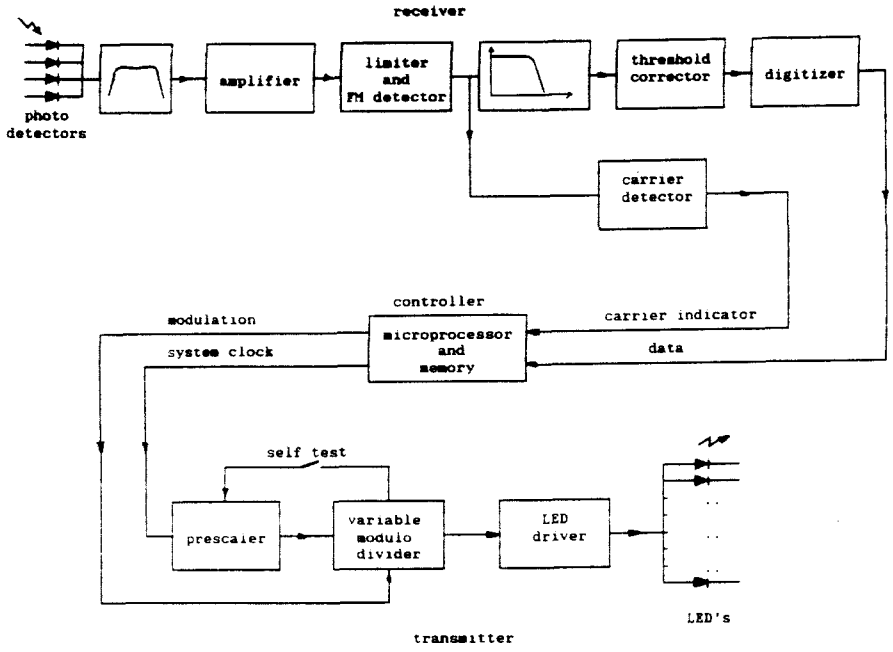

OptoNet tranceiver unit

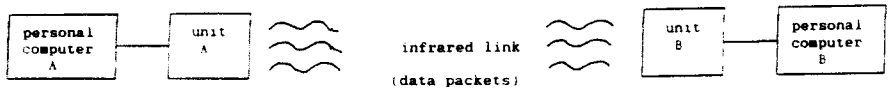

Fig 5.3
Block diagram of OptoNet

5.4 Controller

The IR transmitter and receiver is controlled by a microcontroller system. Intel's 8044 is used as the CPU. With its built-in SDLC data link controller, an error controlled data link is easily implemented. There are 32k

bytes of RAM space shared by program and data. A 32k ROM serves as the fixed program memory, containing an operating system. The device interfaces to a user thru the serial port, and is able to download program/data from the serial port to the 32k RAM.

5.5 Test Results

Packetized data communication experiments have been conducted with the above mentioned system using two identical units of OptoNet, unit A and unit B. The test environment was a large (20 by 50 meter) office room with a light grey, non-glossy ceiling about 3 meters high. The floor was dark grey carpet. The following tests were included:

1. Range vs Transmitter Orientation;
2. Range vs Receiver Orientation;
3. Range vs optical power;
4. Error rate vs distance.

In 1), 2) and 3), 219 data packets, each containing 54 bytes of 8-bit serial data were sent from unit A to unit B. The threshold range was reached when data errors sharply increased as the distance was increased.

5.5.1 Range vs Transmitter Orientation

In this test, the transmitter was rotated 8 times at 45° increments to determine the range vs device orientation. The results are tabulated in Figure 5.4.

Unit A transmitting

orientation	range
0°	13.5m
45°	12.0m
90°	10.0m
135°	11.5m
180°	11.5m
225°	11.5m
270°	10.5m
315°	12.5m

Unit B transmitting

orientation	range
0°	11.0m
45°	10.5m
90°	10.0m
135°	11.0m
180°	11.0m
225°	10.5m
270°	10.5m
315°	10.5m

Fig 5.4

Measurement of range vs transmitter orientation

The directions of the 8 LEDs on each unit were adjusted later. The ranges after the adjustment were 12 meters from A to B and 10.5 meters from B to A (at 265mW sine wave optical output.

5.5.2 Range vs Receiver Orientation

In this test, the receiver was rotated 8 times at 45° increments to determine the range vs device orientation. The results are tabulated in Figure 5.5.

Unit A receiving

orientation	range
0°	10.5m
45°	10.5m
90°	10.0m
135°	10.0m
180°	10.5m
225°	10.5m
270°	10.5m
315°	10.5m

Unit B receiving

orientation	range
0°	12.0m
45°	11.5m
90°	11.0m
135°	12.0m
180°	12.0m
225°	11.5m
270°	11.5m
315°	11.5m

Fig 5.5

Measurement of Range vs Receiver Orientation

5.5.3 Communication Range Test

After the uniform directional distribution was obtained in last test, the curve of range vs emitted optical power was measured. Figure 5.6 shows the locations of the units within the room and how units were moved to vary the distance. The output power levels were set by varying resistors in the LED drivers to control the on-state driving current. The results are tabulated in Figure 5.7. The results are also plotted in Figure 5.8 to compare with the theoretical calculation.

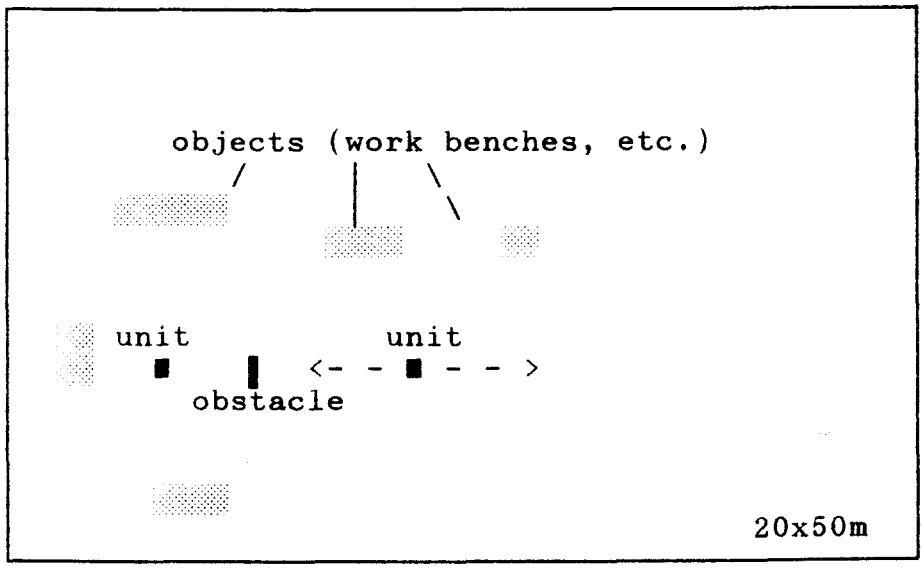

Figure 5.6
Locations of unit A and unit B in the range test

Peak current (mA)	Optical power (mean value) mW	Range (m)	
		A transmits	B transmits
14.0	8	0*	0*
24.5	14	2.3	2
50.0	29	4.5	4
95.0	55	7.5	6.5
190.0	109	9	7.5
461.0	265	12	10.5

* a distance of 0 to 1 meter did not make obvious difference.

Fig 5.7

OptoNet range vs optical power

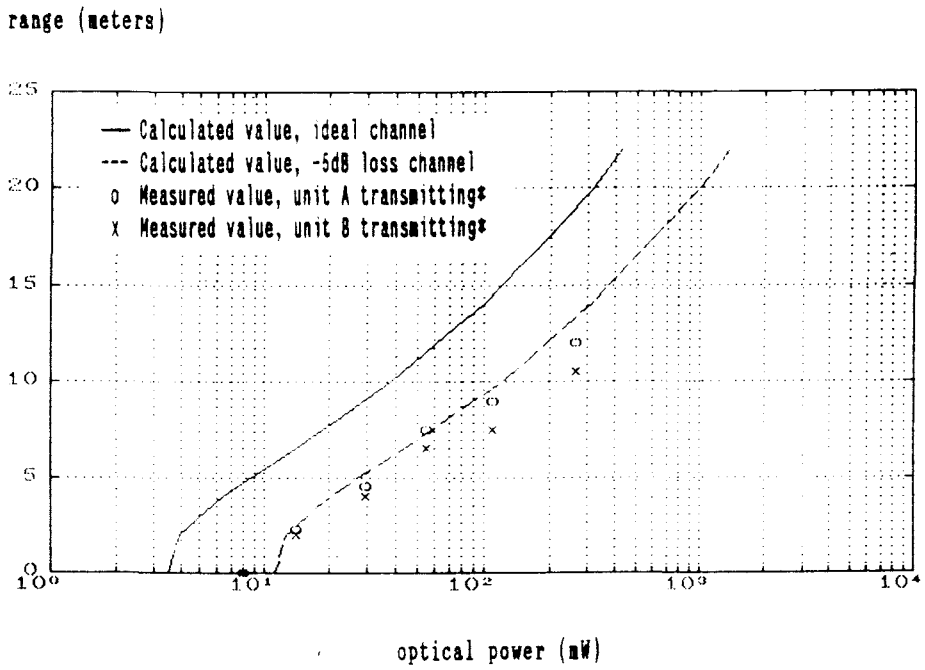

Fig 5.8

Comparison of theoretical range and measured range

In the above test the optical power values were set by setting the driving current of the LED's which have specified power transfer ratio of 0.2mW/mA. Although the transfer ratio has tolerance, the average power transfer ratio of the 8 LED's can be considered quite close to the mean value. A more accurate plot which shows the effect of component tolerance is shown by Figure 5.9, in which the range is plotted against the on-time (or peak) LED driving current. A typical tolerance of ±10% is assumed.

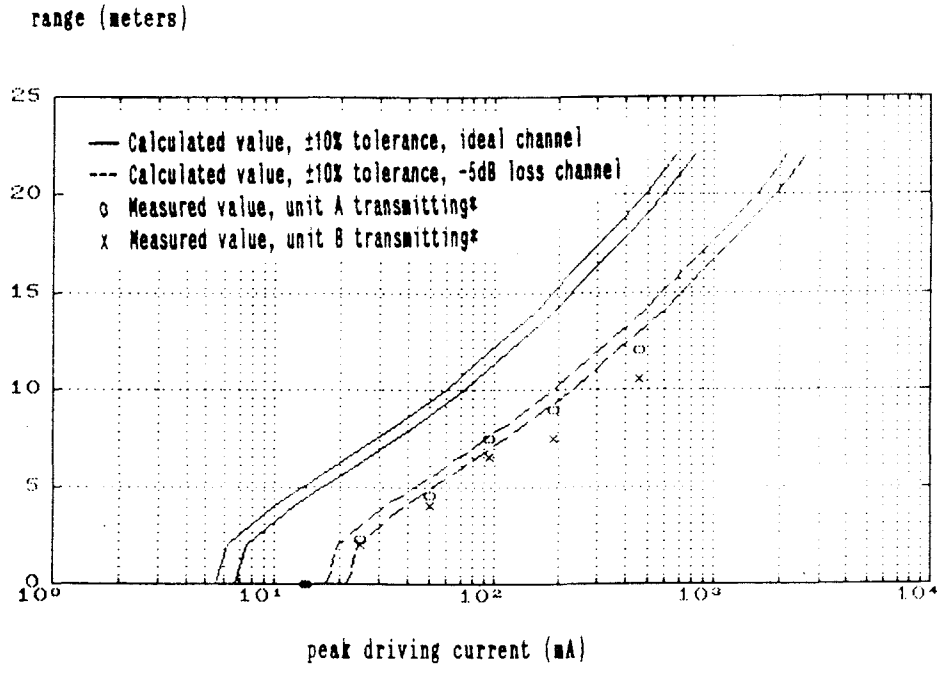

Fig 5.9

Comparison of theoretical range and measured range (component tolerance considered)

5.5.4. Error Rate Test

In the error rate test, communication error rates were determined versus distance. Unit A was used as the transmitter. Figure 5.7 lists the test data. In each measurement 219 packets were sent.

Distance	Valid packets received
0m	219
..	..
12m	219
12.5m	192
13m	44
14m	0

Fig 5.10
Valid packets versus distance

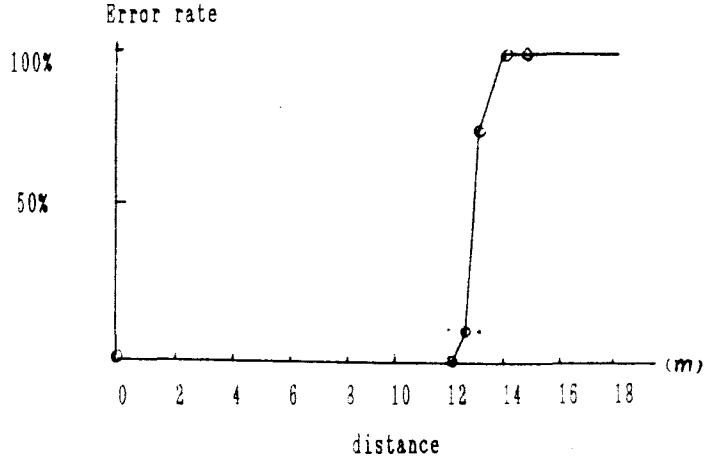

Fig 5.11
Error rate versus distance

5.6 Analysis of Test Results

1. Both the transmitter and receiver presented good directional characters. By properly adjusting the orientaion and angles of the LEDs, very uniform distribution of optical power can be achieved.

2. At larger optical power levels, the curve of range vs optical power agrees with the analytical curve very well (Figure 5.8) . The range is some what below expected values. This could be caused by some of the following reasons: the transmitter was not working at maximum efficiency point (see section 5.2); The design of the receiver is not optimal; The assumptions used in the calculation differ from actuality; etc.

The discrepancy at lower power level is most likely to be caused by the extra amount of reflected power from the surrounding objects.

The experimental curve bent down a little at larger power. This was possibly caused by the temperature rise of LEDs at larger drive. LED output power degrades as temperature rise [11].

3. The different performance of the two units can be explained by the parameter variations among electronic components. Initially, unit A had a much worse performance. It was found out later that the microprocessor on the unit A board generated higher levels of RF interference which caused a degradation in the SN ratio. After shielding the front-end circuit with a metal sheet, most of the interference was eliminated and unit A's performance was improved greatly.

4. The sharp increase of error rate beyond a certain distance suggests that little can be done in software (such as error control/repeated transmissions, etc.) to extend the range considerably. The reason behind this sharp increase of error is due to the FM modulation's threshold effect. Detailed analysis on FM threshold effect and threshold curves can be found in [14].

CHAPTER SIX
SUMMARY

6.1 Achievements

In conclusion, this thesis work showed that the ONP system, a potentially useful and cost-effective communication facility, is feasible and demonstrated experimentally that such systems are practical. ONP systems are suitable in applications where localized wireless and omnidirectional data communications are desired. These may include hospital, restaurant and offices, etc. In large floors such as factories, omnidirectional ceiling repeaters may be required.

The achievements of this research work are summarized as follows.

1. Illumination Functions

Almost all existing optical communication systems are focused (or semifocused), direct-path systems (FDP systems). The optical coupling in a FDP system is relatively efficient. In an omnidirectional, non-direct path (ONP) system, optical signals are spread all over the room. Line-of-sight transmission of light is not assumed. This results in very poor optical coupling between the transmitter and the receiver.

In order to study the feasibility of ONP systems, quantitative analysis is required. This was done by first deriving illumination functions. The illumination function

of a DP system is an optical power density function of distance between the transmitter and the receiver, the total emitted optical power and the cone angle of the light beams. The illumination function of a ONP system is an optical power density function of the distance, the height and reflectance ratio of the ceiling and the total emitted optical power. Comparison of the illumination functions of FDP and ONP systems reveals that the optical signal strength of a ONP system is several thousands times lower than that of a DP system under typical conditions.

2. Feasibility of ONP systems

The illumination of the ONP system is then used to calculate the amount of optical power that a photo detector can pick up at distance. The random noise in a photo detector determine the minimum required optical signal power incident to the detector. A minimum signal-to-noise (SN) ratio is required by the signal processor to recover the signal. This yields a maximum communication distance. Under typical conditions, the theoretical ONP communication range is approximately 10 meters with a few infrared LEDs operating simultaneously. This suggests that ONP systems are feasible.

3. Optimal LED Driving Conditions

The optical power efficiency directly affects the feasibility. Poor efficiency would result in using more optical electronic devices. In order to reach the highest optical power efficiency, driving methods for the LEDs driver were studied. It was shown that the transmitter's optical-electrical efficiency is a function of α, the normalized carrier frequency, and β, the duty cycle of the driving current. There exists a set of optimal (α,β)

pairs. Graphical and analytical methods were worked out which can be used by designers to achieve highest transmitter efficiency.

4. System Level Considerations

The key in designing a receiver is to have a good signal-to-noise ratio in order to extend the communication range with an existing signal illumination. Because an optical receiver is very similar to a radio receiver in nature except for the energy transducer, RF theories and technologies can be readily used in the design of an optical receiver. The particular problem in an optical receiver is to choose good optical detectors (with low noise), and match it to the front-end amplifier. In choosing the carrier frequency, the spectral range containing most of the ambient optical noise should be avoided. The transmitter efficiency should also be taken into consideration, since it is a function of carrier frequency. There is usually a trade-off.

5. ONP Optical Communication Experiment - OptoNet

The practicality of the ONP optical data communication was demonstrated by a successful experiment with OptoNet, a simple ONP system. The system used low-cost electronic components to implement two identical microprocessor controlled units. Frequency modulation was used. 8 infrared LEDs were used on each unit. The test results closely agreed with the analytical results. An omnidirectional and non-direct path range of 12m was recorded with a data rate of 3200 bit/sec.

6.2 Suggestions for Further Work

Some interesting tests and work have not been done. They are either beyond the scope of this study or the limitation of the resources available to the author at the time of experiment. These are listed as follows:

1. The measurement of the illumination function for the omnidirectional and non-direct path system. This is the direct approach to verify the function. In the author's experiment, the illumination function is indirectly verified by measuring the range. The complete measurement, however, requires a highly sensitive infrared optical power meter and a large empty room.

2. The relationship between range and data rate. Theoretically the SN ratio of the receiver is inversely proportional to the square root of signal bandwidth if the channel is also matched to this bandwidth. Therefore the range would decrease with increased signal bandwidth. The test requires the system's ability to change the transmission data rate, the bandwidth of the front-end filters, the detection slope of the FM detector and the bandwidth of the data (audio) filter.

A rough estimate of data rate can be estimated, though. Because their slow rise/fall time, high power infrared LEDs can be driven by carrier frequencies no higher than 1MHz or so. Their maximum data rate is limited by the highest modulating frequency. This is roughly 100kHz. The communication range would be very small at this data rate.

3. The scope of this study was to analyze and verify the feasibility of the omnidirectional, non-direct path

optical data link. The application of such data links may include the local area network. In a network environment, many units would share the same data path (the infrared carrier). The CSMA network protocol [16] would be suitable with modifications. Many problems in such a wireless system resemble those in a radio communication network, hence the protocols used in the various radio networks may be referenced.

The other networking approach is to assign different carrier frequency channels to different units. There would be more than one "bus" in this approach. The number of channels, however, is quite limited due to the low carrier frequency. For example, only about 10 channels could be used for such a system implemented by OptoNet units, since each channel would occupy 40kHz channel capacity.

REFERENCES

1. *MacWorld* , Sep. 1989

2. *Optical Components Databook* , III-V Systems, 1989

3. Ely E. Bell, "Radiometric Quantities, Symbols and Units", *Proc. IRE, 47*, 1432 (1959).

4. C. S. Williams and O. A. Becklund, "Optics: a short course for engineers & scientists, Robert E. Krieger Publishing Company, 1984.

5. A. V. H. Masket, *Tables of Solid Angles*, TID-14975, University of North Carolina, (Available from Office of Technical Services, Department of Commerce, Washington. D.C., $5)

6. *IES Lighting Handbook*, Fourth Edition. Illumination Engineering Society, 345 E. 47th St., New York, 10017, 1981.

7. Henry W. Ott, "Noise Reduction Techniques in Electronic Systems", John Wiley & Sons Publishing, 1976.

8. *NEC Optoelectronics Products*, NEC Corp., 1988

9. A. B. Carlson, "Communication systems", McGraw-Hill, 1975

10. B. P. Lathi, "Modern Digital and Analog Communication Systems," CBS College Publishing, 1983.

11. "Opto Electronics Data Book", Copyright 1988 Opto Diode Corp.

12. A. B. Carlson, "Communication Systems,"
McGraw-Hill, 1975.

13. H. S. Black, "Modulation Theory", Copyright 1953 by D. Van.
Norstrand Company, Inc.

14. A. B. Carlson, "Communication Systems,"
McGraw-Hill, 1975.

15. D. Liu, "Ambient Near Infrared Energy Measurement", EE563 Course
Project, 1988, E&CE Department, Oregon State University 15.

16. Tanenbaum, A. S., *Computer Networks*, Prentice-Hall,
NJ., 1981